NAVWEPS REPORT 7808
NOTS TP 2806
COPY 30

EXPERIMENTAL DETERMINATION OF PRESSURE DISTRIBUTION ON A SPHERE DURING WATER ENTRY

by
C. R. Nisewanger
Underwater Ordnance Department

ABSTRACT. The pressure distribution on a 12-inch-diameter sphere during vertical water entry at 23.5 fps was determined by direct pressures versus time measurements at several points on the sphere.

From these data, pressure versus angle from the stagnation point was plotted for various penetrations; the rise of the free surface of the water versus penetration was determined; and the drag coefficient versus penetration was ascertained by graphic integration of the pressure-distribution curves and by acceleration measurement.

The results are compared with some theoretical curves.

U.S. NAVAL ORDNANCE TEST STATION
China Lake, California
27 October 1961

CONTENTS

NOMENCLATURE

a	Acceleration
A	Cross-section area of sphere
b	Penetration below undisturbed water surface in radii of sphere
b_1	Effective penetration below actual water surface in radii of sphere
C_D^*	Drag coefficient, dimensionless
d	Distance from pivot to vertical axis of sphere
D	Drag force
h	Rise of free surface in radii of sphere
I	Moment of inertia of sphere and arm apparatus about pivot
P	Instantaneous pressure during entry
P_α	Pressure at angle α
R	Radius of sphere
t	Time
t_o	Instant sphere contacts water
V	Velocity of sphere
V_o	Velocity of sphere at t_o
α	Angle from stagnation point
α_e	Angle from stagnation point to edge of experimental wetted arc
α_g	Angle from stagnation point to gage center
α_u	Angle from stagnation point to edge of wetted arc for undisturbed water
θ	Azimuth angle
ρ	Density of water

INTRODUCTION

An experimental research program was undertaken to obtain pressure-distribution data for typical missile nose shapes and entry conditions. Considerable theoretical work had been done (Ref. 1 to 4) and measurements were needed to evaluate the results in terms of experimental evidence.

The first phase of the program was designed to develop suitable pressure transducers and techniques to record the extremely fast-rising transients. Most of this development work, completed by 1951, is reported in the Appendix (originally published as Technical Memorandum 614). Another pressure transducer, described in this report, was developed later.

In the second phase, experiments were performed in which a 12-inch-diameter sphere was instrumented with a small, fast-response pressure transducer or gage that could be placed at any one of several points on the sphere surface. As the sphere dropped vertically into the water, a signal from the gage was displayed on an oscilloscope and photographed. Pressure versus time records were thus made for each point, and from these records the pressure distribution, the rise of the free surface, and the drag coefficient were obtained. The signal of an accelerometer, mounted in the sphere, provided an independent determination of the drag coefficient.

The study was discontinued before all objectives were achieved, and the data, though significant, are not complete.

APPARATUS

Figure 1 is a general view of the experimental setup showing the sphere (actually a hemisphere) mounted on a pivoted arm that is raised and released to let it fall into the water. After the desired penetration, the arm is arrested by sponge-rubber bumpers. Although the path of the sphere is an arc, the direction is vertical at impact, and the change in direction is negligible during the penetration of interest.

The recording equipment, including oscilloscope, camera, and preamplifier, is shown in the foreground of Fig. 1. Instrument cables run from the sphere along the arm to the hinge and then to the recording equipment.

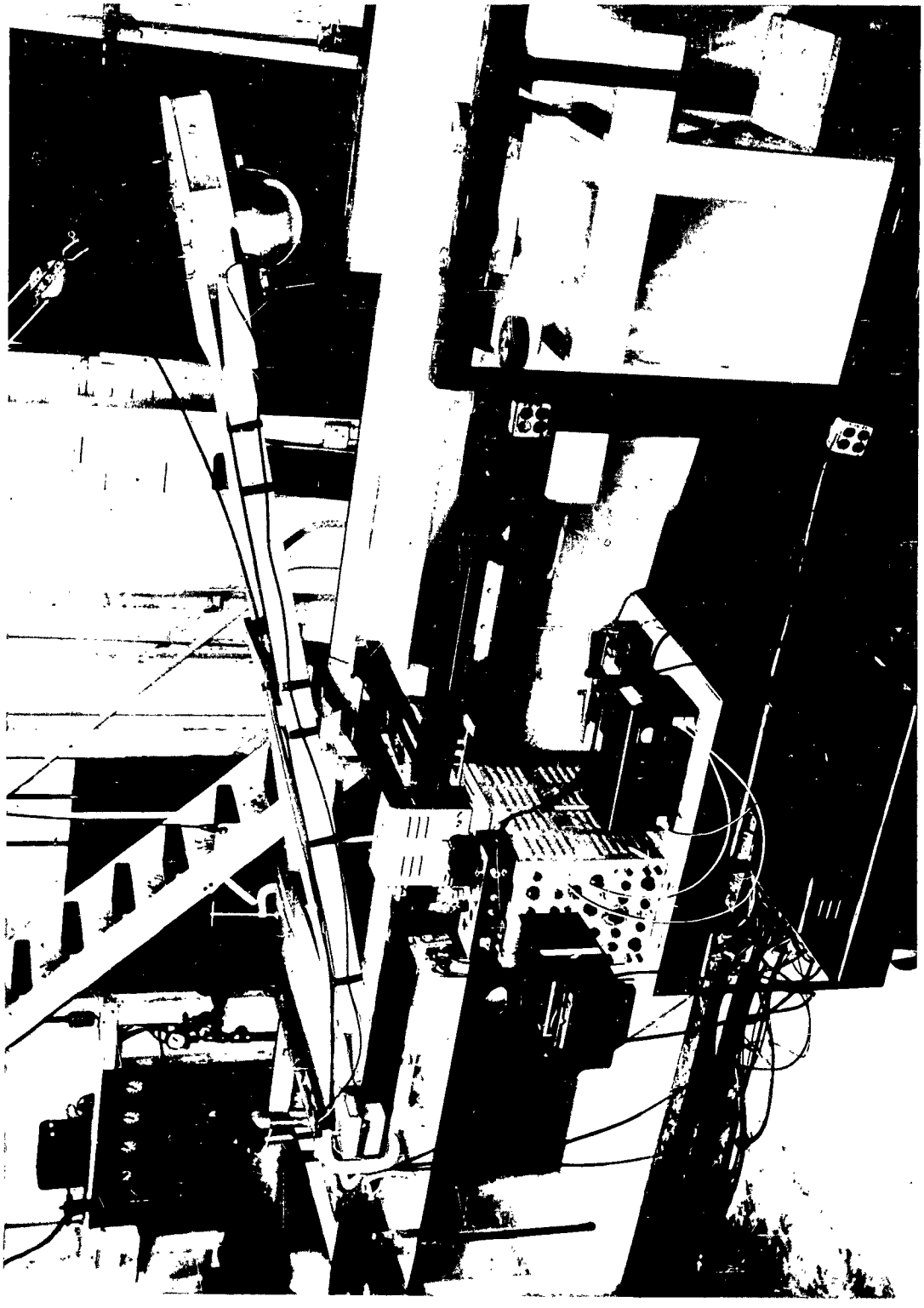

FIG. 1. Experimental Setup.

THE SPHERE

The sphere is 12 inches in diameter with a 1-inch wall turned from 24ST aluminum alloy. Three different spheres were used to cover the range of angles over which measurements were made. Each one had the gage mounted at a different angle from the stagnation point: 0, 10, and 30°. In order to obtain intermediate angles, the sphere mount was adjustable in small increments through a range of approximately 16°.

Two insulated probes were also mounted on the arm, used as switches to close electrical circuits on contact with the water surface. Some electrolyte was added to the water to increase its conductivity. One probe contacted the water ahead of the sphere to start the oscilloscope sweep; the other contacted it later to produce a fiducial mark on the timing records at a preset time relative to the instant the sphere touched the water, t_o, which was also electrically determined by allowing the sphere to close a circuit upon contact with the water. This makes it possible to correlate the pressure records for the various points on the sphere with respect to t_o.

THE GAGES

All records except those of the initial portion of the stagnation point transient were made with the wafer gage shown in Fig. 2. The sensitivity of this quartz gage is 0.74 $\mu\mu$ coulombs/psi, and the natural frequency is about 500 kc. The extremely fast pressure rise at and near the stagnation point excites the natural frequency of the gage to large amplitudes, rendering the records useless until the inherent damping reduces the ringing amplitude to a low level. Low-pass filters, used with discretion, improved the records and yielded useful data for all but the first few thousandths of a radius of penetration.

Useful stagnation-point data from a penetration of 2×10^{-4} radii to about 10^{-2} radii were obtained with the rod gage shown in Fig. 3. This gage, described in detail in the Appendix, has a radial mode of about 500 kc. The lower limit of penetration for which the gage is useful is not necessarily due to the gage response time, but may be attributed to the penetration required to immerse the gage face (explained later). The upper limit of penetration for which the gage is useful is determined by the gage length, which determines the time for the elastic wave initiated in the rod by the pressure to traverse the length of the rod, to reflect, and return to the quartz. This takes about 200 μsec for the 23-inch rod.

Each gage was calibrated against a laboratory standard Bourdon gage, as follows. A fast-rising pressure step was applied to the gage through a quick-opening valve connected to a reservoir of air at a known pressure measured by the Bourdon gage. The pressure-step signal on the oscilloscope was compared to a similar "Q-step" signal

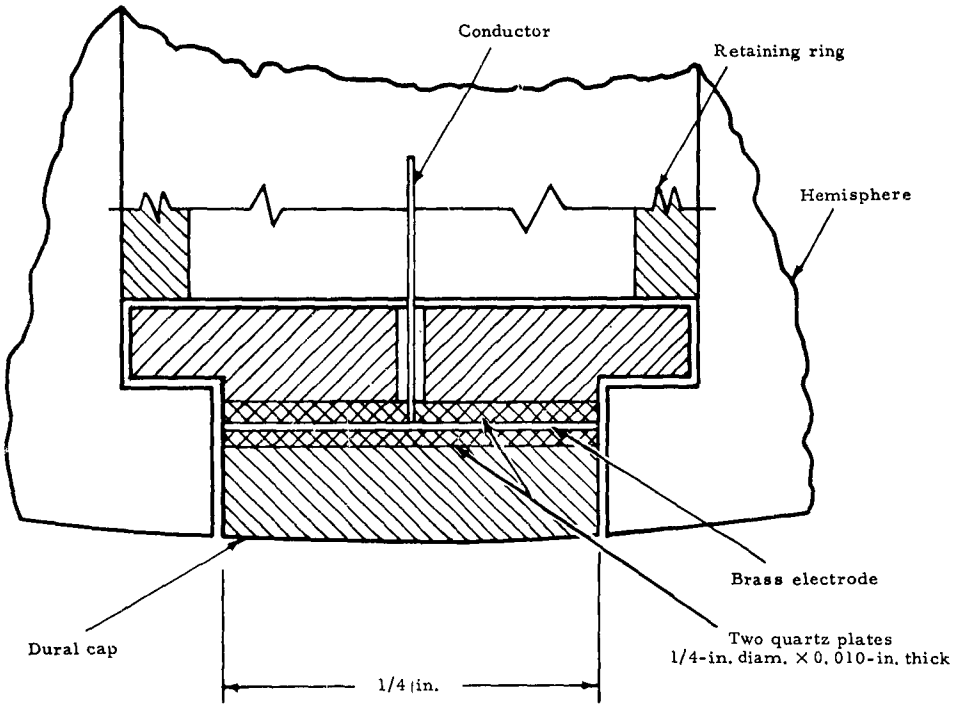

FIG. 2. Wafer Gage.

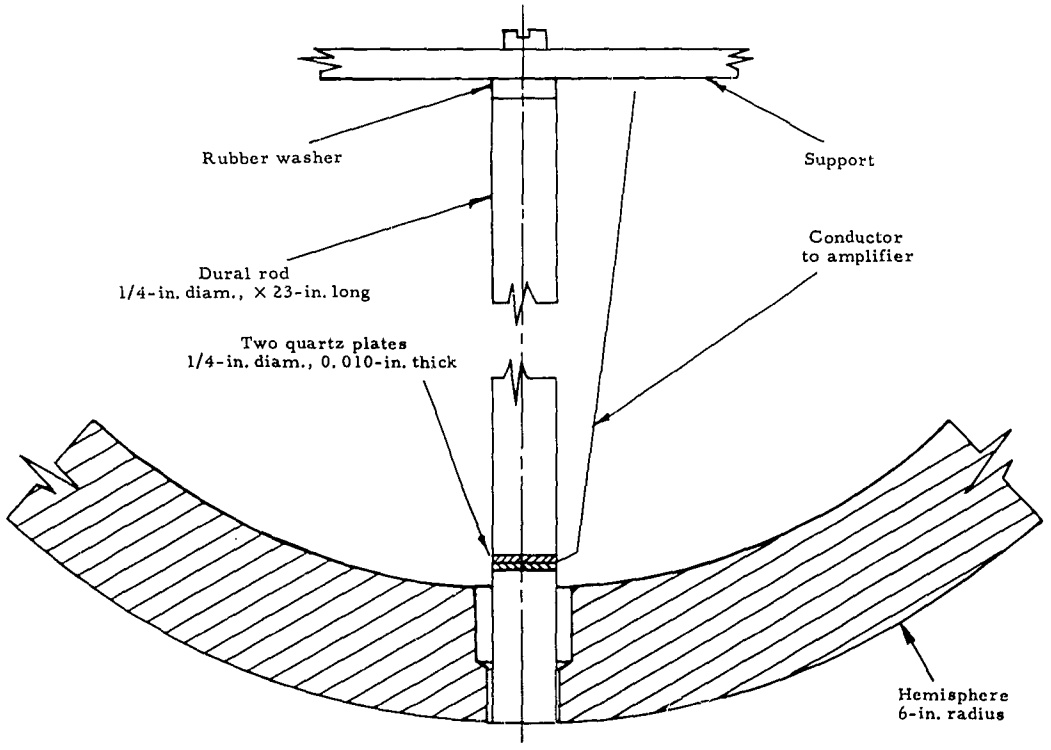

FIG. 3. Rod Gage.

produced when a switch is closed, charging the gage with a known electric charge from a calibrated condenser.

The dynamic response of each gage was determined by the shock-tube technique described in the Appendix, in which a true pressure-step was applied to the gage, causing it to ring. The signal was displayed on the oscilloscope and photographed for detailed examination.

Significant complications have arisen because the gages do not measure pressure at a point, due to their finite diameter. They actually measure the total force on the gage face, and when the face is totally immersed, the force divided by the gage area yields the mean pressure, assumed within the experimental error to be the pressure at the center of the face, even though a gradient exists across it. However, the face is not totally immersed instantaneously. The 1/4-inch-diameter spherical face subtends an arc of 2.39°. After the lowest point on the face touches the water, an additional penetration, Δb, is required to immerse it completely. For a gage centered at the stagnation point, $\alpha_g = 0$, the additional penetration, assuming an undisturbed flat water surface, is $\Delta b = b = 1 - \cos 1.19^{\circ}$, since the center of the gage touches first. For a gage centered at α_g, equal to or greater than the gage half-angle 1.19°, the additional penetration is $\Delta b = \cos (\alpha_g - 1.19^{\circ}) - \cos (\alpha_g + 1.19)$. Thus Δb varies from 2×10^{-4} radii for the gage centered at $\alpha_g = 0$ to 25.8×10^{-3} radii for the gage centered at $\alpha_g = 38^{\circ}$. Therefore, the gage does not resolve the initial fast pressure rise or record the true peak-pressure, but yields valid results only after the additional penetration required to completely immerse the face.

The relationships above do not yield the precise values for Δb since the water surface does not remain flat but rises around the sphere. The penetration for complete immersion of a gage centered at any angle can, however, be experimentally determined, as will be shown later.

GAGE INSTALLATION

The necessity for maintaining a smooth spherical surface across the gage face and the adjacent area is discussed in detail in the Appendix. This critical requirement was met by precisely adjusting the spherical gage face so that it was flush with the surface of the sphere and covering it and the surrounding area with cellophane tape. The tape was smoothed with abrasive paper, sprayed with several coats of lacquer, and the surface rubbed after each coat to obtain a smooth finish.

THE ACCELEROMETER

For the acceleration measurements, the pressure gage was removed, the hole in the sphere plugged, and the surface carefully contoured.

A piezoelectric accelerometer with a quartz element was mounted on the inner surface of the sphere just above the stagnation point. The accelerometer signal was recorded with the same apparatus that was used for recording the pressure signals.

The instantaneous local pressure integrated over the wetted area during water entry results in a drag force which gradually increases from zero at the instant of contact to a peak value at a penetration of about 0.15 radii, then slowly decays to the steady-state drag. For an entry velocity of 23.5 fps, the rise time is about 3×10^{-3} seconds. Therefore the accelerometer, with a natural period of about 2×10^{-4} seconds, has adequate response to record the transient. However, the local pressure at the stagnation point rises instantaneously (theoretically) to a high value on contact (like a hammer blow). This produces a high, steep strain wave in the metal that propagates through the accelerometer and excites its natural frequency to a high amplitude, just as it does in a pressure gage. To obtain a usable record it is necessary to employ a filter to attenuate the accelerometer-ringing frequency and yet provide an adequate bandwidth to properly pass the acceleration transient.

RESULTS

PRESSURE VERSUS PENETRATION

Figure 4 shows typical pressure versus time records made at $\alpha_g = 8^\circ$. Timing marks on the base line are 100 μsec. A preliminary timing run is shown at Fig. 4A. The pips mark the water contact; the smaller pip the probe, and the larger pip the sphere. Figure 4B is the pressure record showing the initial pip caused by the probe contact, followed by the pressure signal. The upper horizontal line is the "Q-step" pressure calibration equal to 100 psi. The gain and the sweep time are increased in Fig. 4C to show the later portion of the transient. The pressure peak is off-scale.

The finite time to peak pressure is due to the time required for full immersion of the gage, and the true pressure is recorded only during the decay portion of the record, after the gage is fully immersed. The slower rising initial toe may be attributed to the compression of air trapped between the sphere and the water, or to the thin sheath of water that rises around the sphere ahead of the "solid" front.

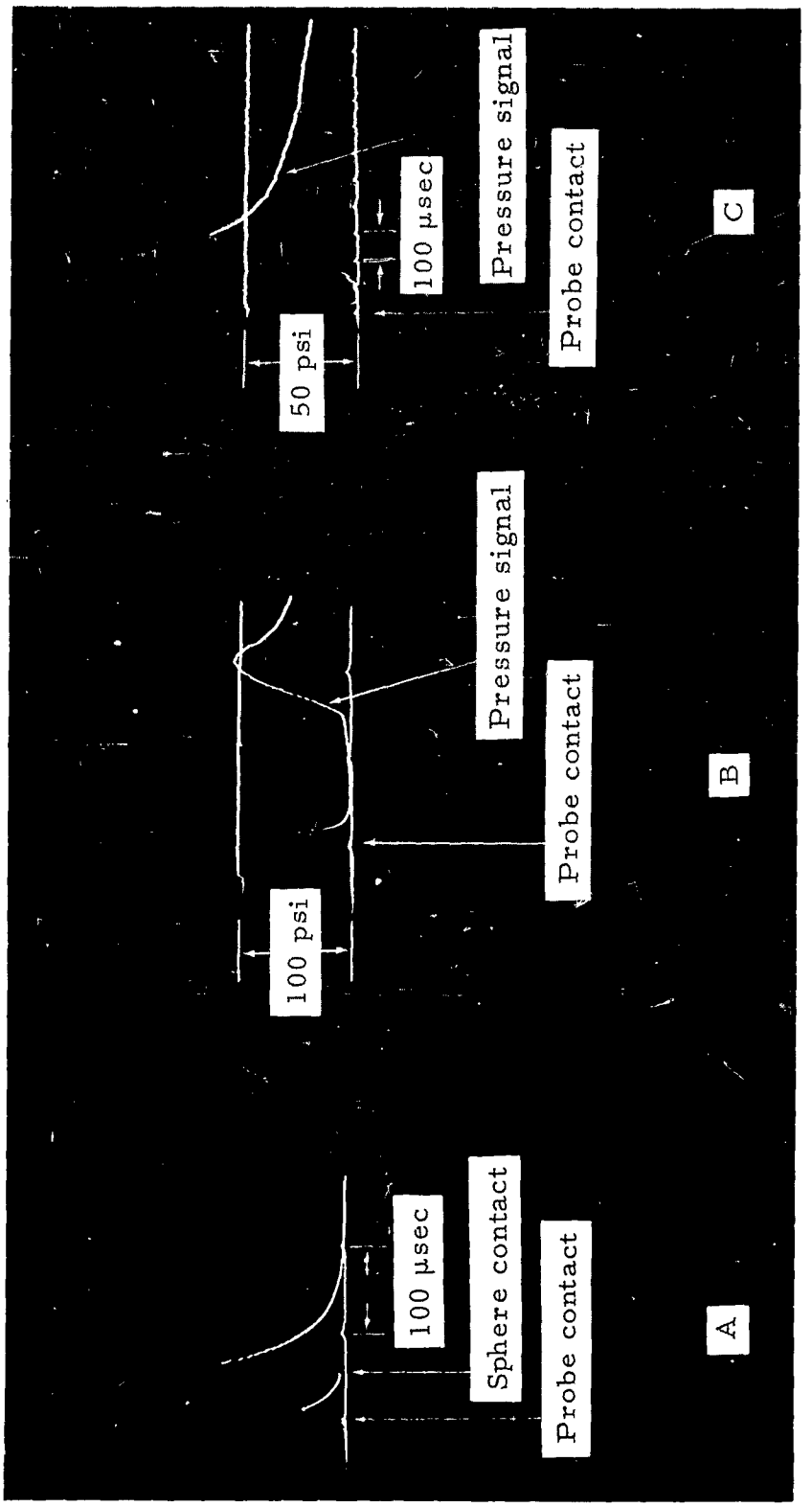

FIG. 4. Pressure Versus Time α_g = 8 Degrees.

Figure 5 shows a typical pressure versus time curve obtained from records made with the wafer gage at $\alpha_g = 22.18^\circ$. Time is measured

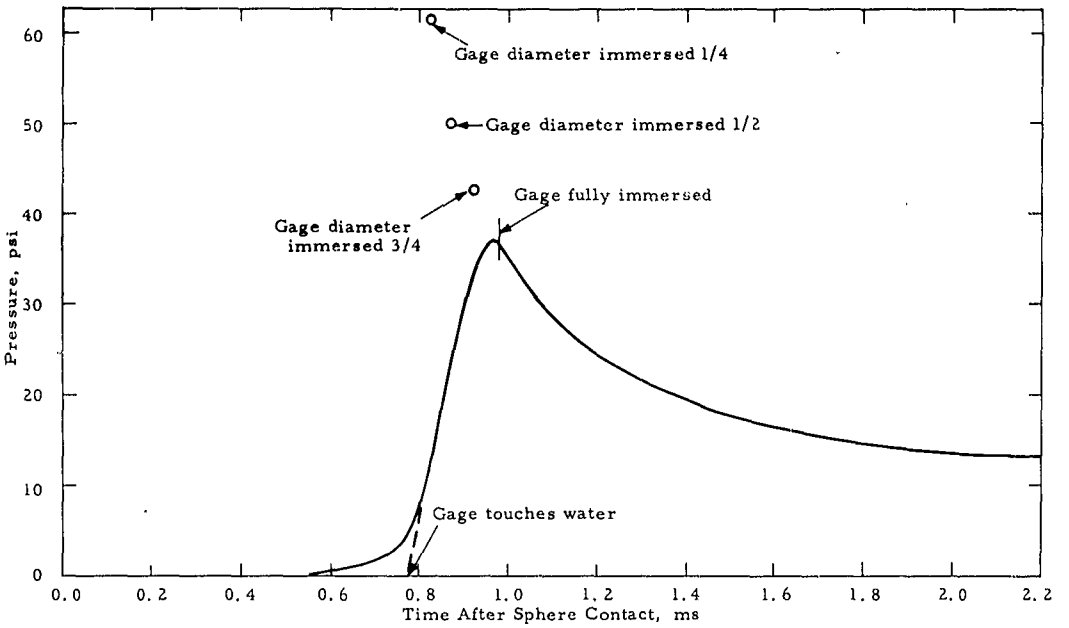

FIG. 5. Pressure Versus Time at $\alpha_g = 22.18$ Degrees.

from the instant of contact and penetration $b = V_o t$, since V does not change measurably during the transient. The penetration for full immersion of the gage is assumed to occur at the inflection point, as indicated by the short vertical mark.

Records obtained with the rod gage at the stagnation point are shown in the Appendix.

To display the complete pressure versus penetration history of the sphere conveniently, the records obtained at all the 10-gage points were plotted on logarithmic coordinates (Fig. 6). The gage points α_g are 0, 3.05, 5.63, 7.37, 8.00, 10.13, 15.82, 22.18, 30.18, and 38.18°. The superimposed oscillations appearing on some of the records were smoothed out and the low-pressure initial toes omitted.

PRESSURE VERSUS ANGLE FROM THE STAGNATION POINT

From the pressure versus penetration curves, plots of pressure versus angle from the stagnation point, α, were obtained for the penetrations at which each gage was completely immersed. These are shown as solid lines in Fig. 7. (Only two gages were immersed for the pene-

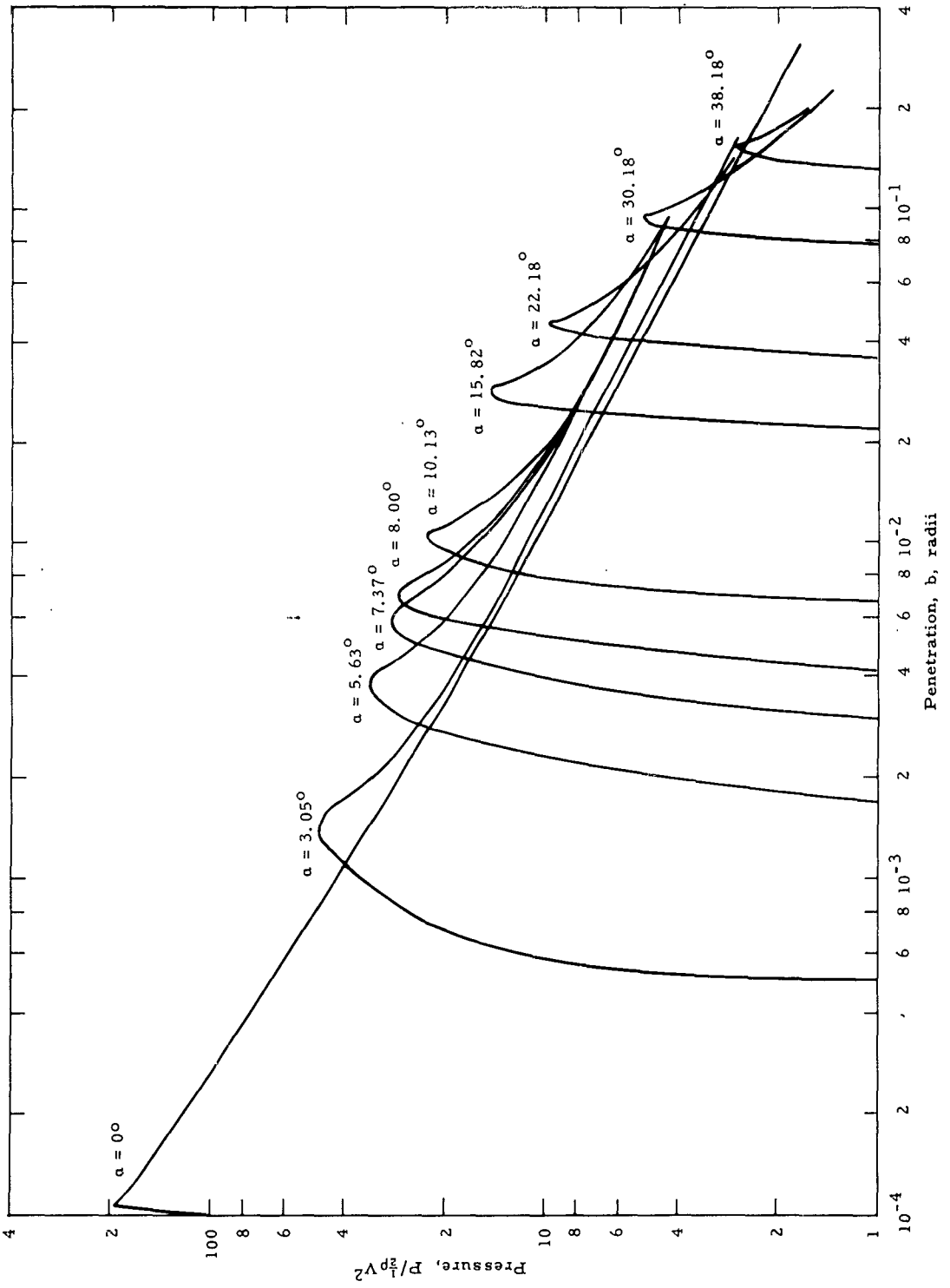

FIG. 6. Pressure Versus Penetration for Various Values of α.

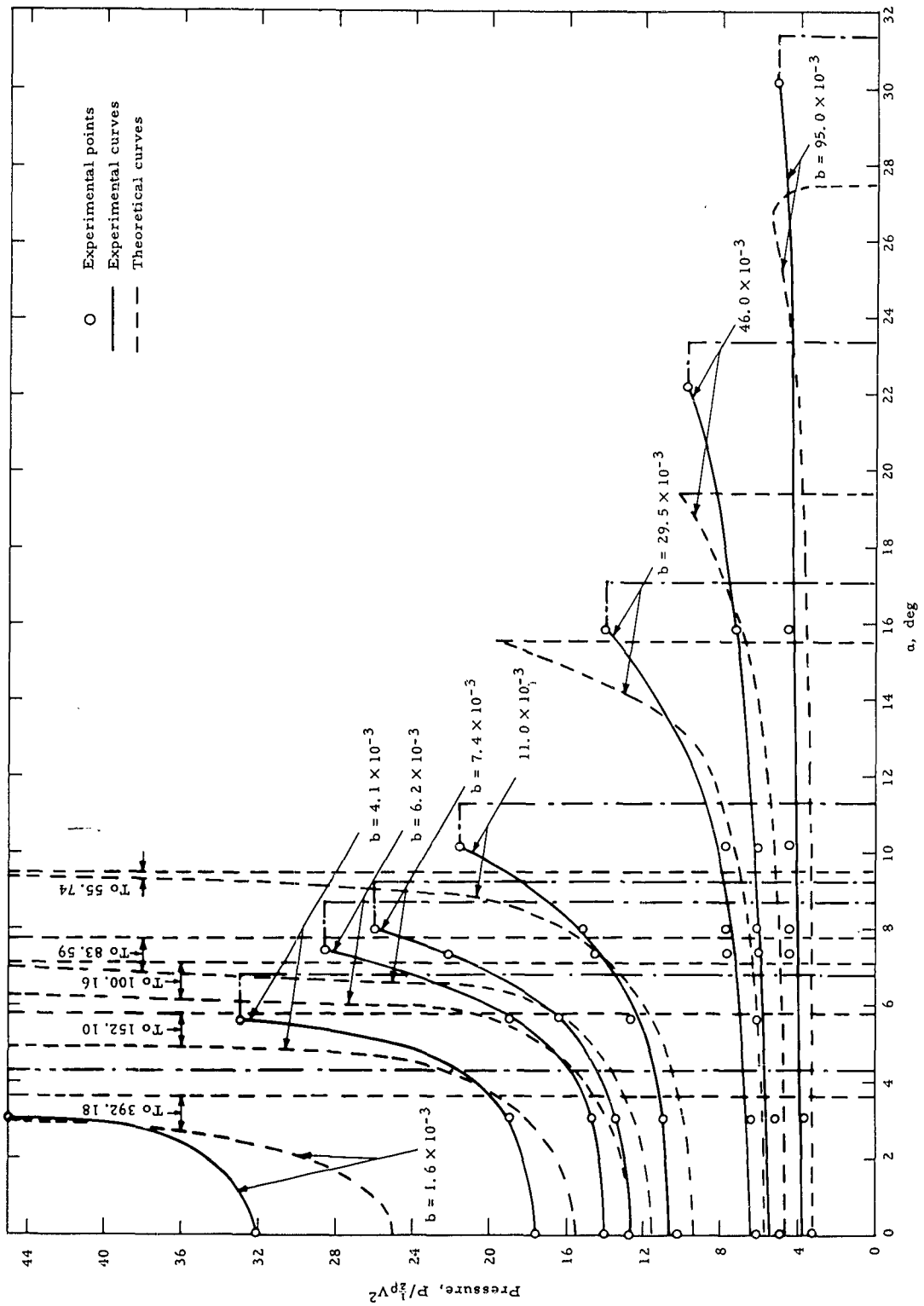

FIG. 7. Pressure Distribution for Various Values of Penetration.

tration of $b = 1.6 \times 10^{-3}$ radii and therefore the curve is not defined.) A zone of undetermined pressure for each penetration occurs in the arc bounded by the edge of the wetted surface and the center of the last completely immersed gage (1.18°, the gage half-angle). This undetermined pressure is shown by a dashed horizontal line extending to the edge of the wetted arc and then falling to zero. The actual pressure is higher since theory predicts maximum pressure very near the edge of the wetted arc, and approximate experimental values can be obtained by making certain assumptions for the partially immersed gage, as will be shown later.

RISE OF THE FREE SURFACE

The rise of the free surface of the water was determined by the following procedures: the penetration at which the lowest point on the gage touches the "solid" water (not the thin sheath) is sharply defined on the records by the beginning of the steep rise following the slowly rising toe (Fig. 4 and 5). Thus, from the pressure versus penetration curves (Fig. 6), the wetted arc versus penetration can be accurately determined for the angles corresponding to the lowest point of each gage (α_g - 1.19°). A plot of these points is shown as α_e in Fig. 8. Since the water surface rises, the experimental wetted arc, α_e, for a given penetration b is larger than it would be for an undisturbed surface where $\alpha_u = \cos^{-1}(1 - b)$, also shown in Fig. 8.

The effective penetration is $b_1 = (1 - \cos \alpha_e)$, and the rise of the free surface is $h = b_1 - b$ or $h = \cos \alpha_u - \cos \alpha_e$.

The ratio $b_1/b = W_b$ is called the wetting factor. Figure 9 is a plot of the experimental values of W_b versus $\sqrt{b}$. The line of least squares fitted to the data is

$$W_b = 1.736 - 0.586\sqrt{b} \tag{1}$$

Substituting the expression for b_1 into Eq. 1, the following equation for α_e is obtained and plotted in Fig. 8.

$$\alpha_e = \cos^{-1}(1 - 1.736b + 0.586b^{3/2}) \tag{2}$$

DETERMINATION OF THE DRAG COEFFICIENT

The vertical component of force on the sphere for any penetration is determined as follows:

The element of surface $rd\theta\, Rd\alpha$ is shown in Fig. 10. Since R is the radius of the sphere and α is the angle from the stagnation point, $r = R \sin \alpha$.

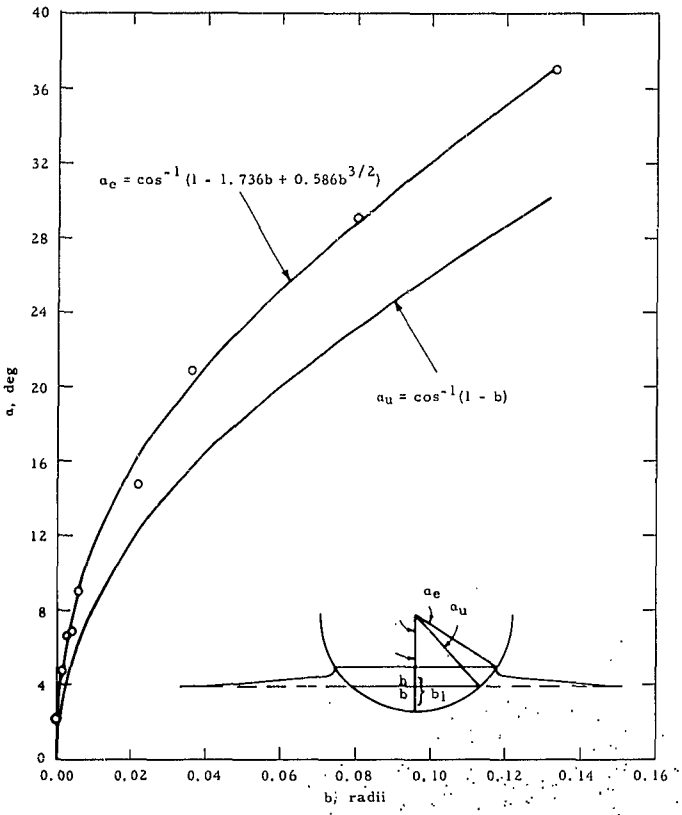

FIG. 8. Wetted Arc Versus Penetration.

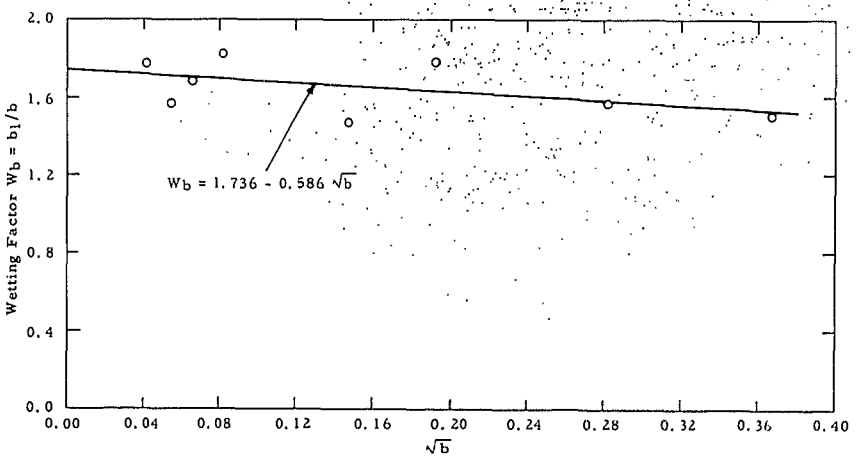

FIG. 9. Wetting Factor Versus Square Root of Penetration.

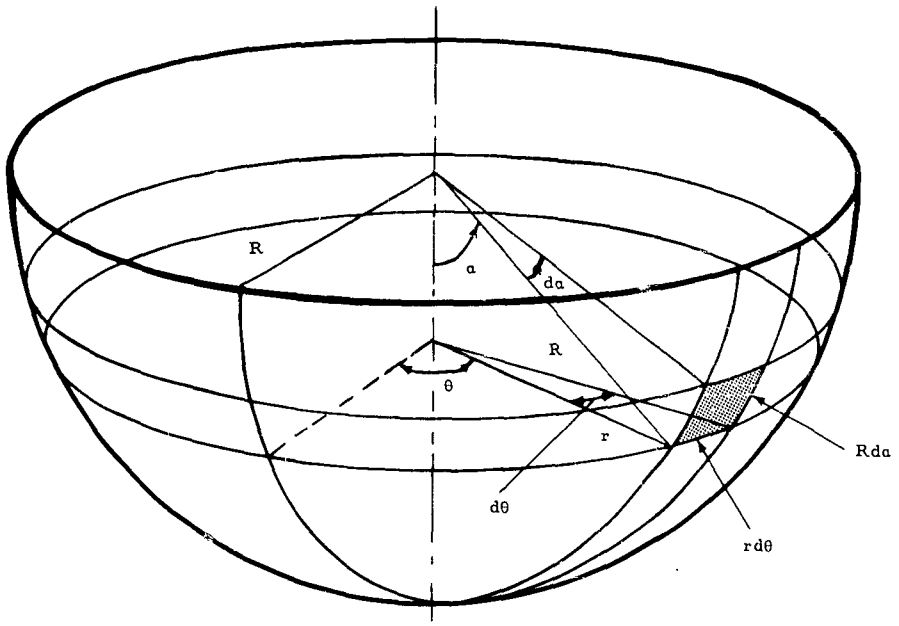

FIG. 10. Surface Element rdθ Rdα.

The vertical component of force on the element is

$$dD = P_\alpha R^2 \, d\alpha \, d\theta \sin\alpha \cos\alpha$$

where P_α is the pressure at the angle α.

The total vertical component of force at any penetration þ is

$$D = \int_0^{\alpha_e} P_\alpha R^2 \sin\alpha \cos\alpha \, d\alpha \int_0^{2\pi} d\theta$$

$$D = 2\pi R^2 \int_0^{\alpha_e} P_\alpha \sin\alpha \cos\alpha \, d\alpha$$

To evaluate the integral, the ordinates of the pressure versus angle curves (Fig. 7) were multiplied by sin α cos α, the curves plotted, and then graphically integrated.

The drag coefficient is $C_D^* = 2D/\rho V_o^2 A$, where V_o is the velocity at impact and A is the cross-section area of the sphere.

The drag coefficient was also determined from the acceleration measurements by applying the relationship $D = Ia/d^2$, where I is the moment of inertia of the sphere and arm about the pivot, a is the

acceleration measured by the accelerometer, and d is the distance from the pivot to the vertical axis of the sphere.

Figure 11 shows the drag coefficients obtained by both pressure and accelerometer measurements and also the theoretical curves of Schiffman and Spencer (Ref. 3) for the sphere at constant-entry velocity.

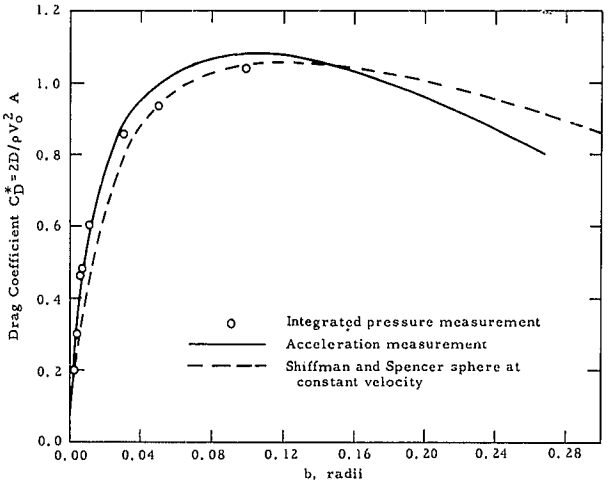

FIG. 11. Drag Coefficient Versus Penetration.

DISCUSSION

The pressure versus time curves are valid (after the gage is fully immersed) to an accuracy limited to the calibration, oscilloscope distortion, and reading accuracies that are estimated to be within ±5% for pressure and ±1% for time.

Full immersion of each gage is assumed to be at the inflection point of the curve, just after the maximum. This assumption was checked by comparing it with the value obtained by adding to the experimental value of b, at which the gage first touches the water, the additional penetration Δb required to immerse the gage. The additional penetration can be read from the experimental curve for the wetted arc versus penetration (Fig. 8) using α_e and $\alpha_e + 2.38^\circ$.

The pressure-distribution curves are valid at the points indicated in Fig. 7. However, for small penetrations there are not enough gage points to define the curves accurately. Also, there is a zone of undetermined pressure between the edge of the wetted arc and the center of the last fully immersed gage.

Although it is impossible to accurately determine from these experiments the pressure near the edge of the wetted arc, an estimate was made of the pressure during the immersion of the gage centered at 22.18°. This was done by assuming that the actual pressure is the indicated pressure divided by the fraction of the gage face area that is wet. The pressures for 1/4, 1/2, and 3/4 of the immersed gage diameter are shown as points in Fig. 5. The previous assumption that the indicated pressure is that pressure at the center of the fully immersed gage is obviously inexact for the early penetration. The exact location of the center of pressure on the gage face is unknown, due to the gradient near the edge of the wetted arc. However, it is initially at the edge of the gage and shifts toward the center as the penetration increases. Thus, a considerable error exists in the pressure versus penetration curves during the early penetration of the gage, and the points indicating the pressure during gage immersion (Fig. 5) must be considered as approximations. Further refinement of these approximations is beyond the accuracy of the measurements.

The values obtained for the drag coefficient as determined by integration of the measured pressure distribution are obviously somewhat lower than they should be, since the pressure values assumed in the zones of undetermined pressure are less than the actual values.

In determining the drag coefficient by means of acceleration measurement, the accuracy is limited, not only by the calibration, distortion, and reading errors, but also by the error in determining the moment of inertia of the apparatus. This is complicated because the flexibility of the pivoted arm tends to isolate the sphere so that it behaves somewhat as a freely falling body. (This flexibility gives rise to the low-frequency oscillations shown in the accelerometer records.) Because of the uncertainties in determining the actual effective moment of inertia of the apparatus, no estimate of the accuracy of the results is presented. Figure 11, however, shows that good agreement is obtained between the two experimental determinations of C_D^*.

CONCLUSIONS AND FUTURE PLANS

The objectives of the study were not fully achieved because the project was discontinued. The major part of the work, the development of suitable pressure transducers, was completed and satisfactory instrumentation produced. The data, though not as complete or as accurate as desired, are significant as a basis for comparison of theory and experiment.

Instrumentation improvement has been achieved since completion of measurements in 1954, with the result that better measurements are now possible. The use of smaller-diameter pressure transducers, an

accelerometer of higher natural frequency, and a linear trajectory for the sphere are the most obvious improvements that could be made. (In the initial work reported in the Appendix, a vertical free fall was used, but the apparatus was not available for the later tests reported here.)

The need for reliable experiments is discussed in Ref. 5 and 6, where it is pointed out that past experimental results were inadequate for evaluating the accuracy of theoretical predictions.

It is now planned to continue experiments using improved techniques at higher entry speeds, and to include measurements on an actual torpedo nose shape.

Appendix

LABORATORY MEASUREMENTS OF PRESSURE VERSUS TIME AT WATER IMPACT[1]

[1] Originally published as Technical Memorandum 614, U. S. Naval Ordnance Test Station, Inyokern, 21 January 1952.

INTRODUCTION

A necessity for additional knowledge of forces acting on missiles during water entry is generally recognized. Some theoretical expressions for the pressure transients at various points on a rigid sphere have been derived (Ref. 1 and 7). Direct experimental information is needed to check the validity of, and if necessary, to modify and extend, the theory. The availability of this information will make possible a direct approach to many of the structural problems associated with missiles; it will also improve the background of ballistic information on air-to-water missiles.

The experimental work is difficult chiefly because of the fast response required of measuring instruments in order to record the transients. The major efforts to date have been the development and testing of instrumentation and the perfection of experimental methods for the attainment of suitable measurements.

LABORATORY APPARATUS

A laboratory setup was established for making direct pressure measurements on bodies by means of electromechanical transducers (hereafter called gages) set flush in their surfaces (Fig. 12). An experimental body, a 12-inch-diameter hollow Dural hemisphere mounted on a suitable carriage, is guided between two vertical rails as it falls from a height of 11 feet into a tank of water. The velocity at impact is 23.5 ± 0.5 ft/sec, and the same velocity was used throughout the experiments. A gage mounted flush in the bottom of the hemisphere is shown in Fig. 12.

The pressure transient picked up by the gage is displayed on a cathode-ray oscilloscope and photographically recorded. Just before the hemisphere strikes the water the oscilloscope sweep is started by means of an electrical impulse which is generated when an insulated probe attached to the carriage contacts the water. Timing markers on the oscilloscope sweep are generated by means of a 10- or 100-kc standard oscillator and pulse-shaping circuit. The hemisphere velocity is measured by means of an electronic timer.

A shock tube (Fig. 13) was installed to check the response of gages (Ref. 8). This device generates a pressure pulse of known shape and magnitude; specifically, a discontinuous pressure step having a flat top of finite duration followed by an approximately exponential decay. It consists of a steel tube $5\frac{1}{2}$ inches in diameter and 13 feet long, closed at the ends by steel plates. A plastic diaphragm is inserted in a flanged joint 2 feet from one end of the tube. At the other end of the tube, gages to be tested are installed flush in the wall or in the end plate. The 2-foot section is filled with compressed air, and the diaphragm is ruptured by means of a cutting mechanism initiating a shock wave that propagates along the tube.

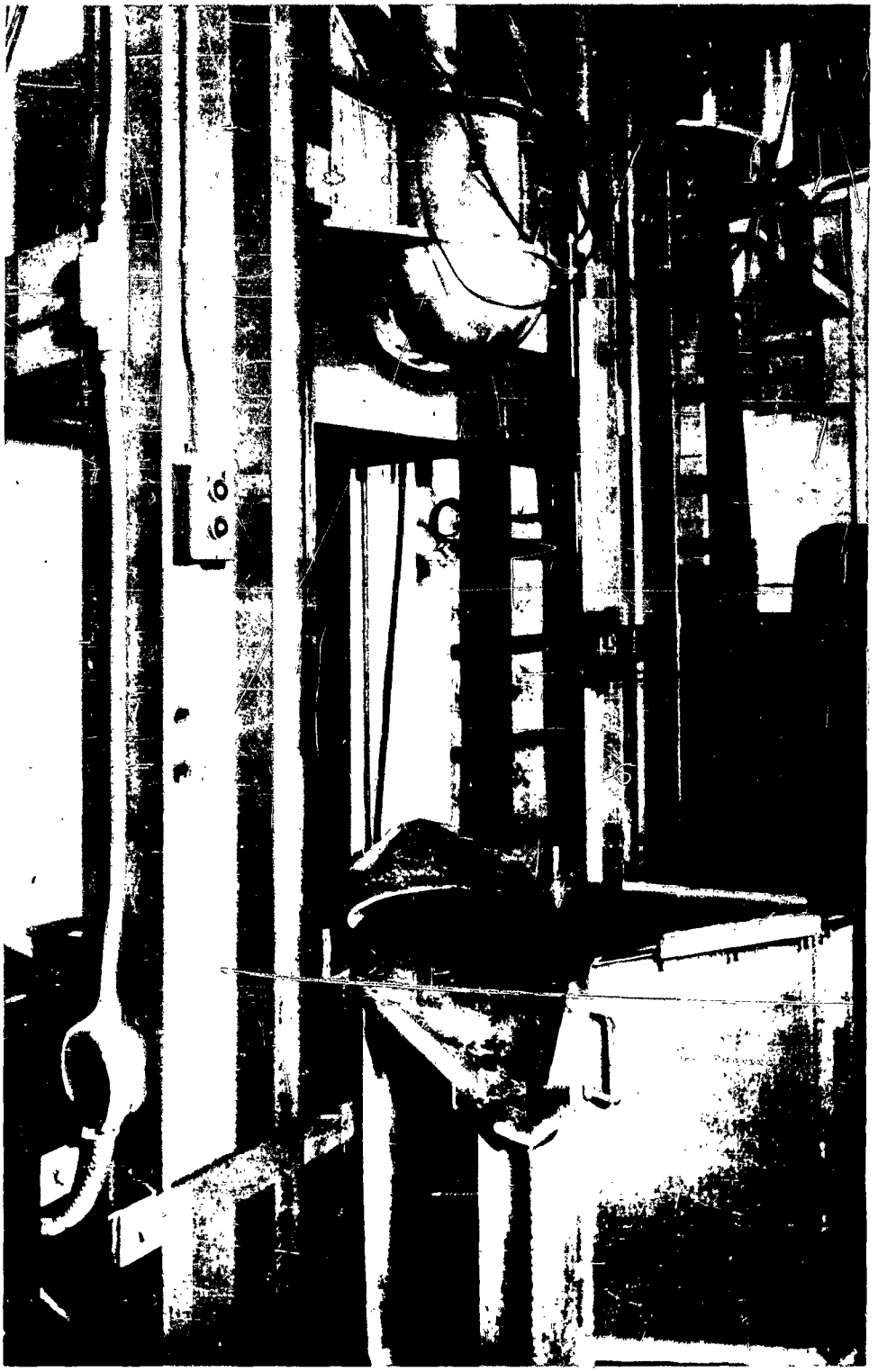

FIG. 12. General View of the Apparatus.

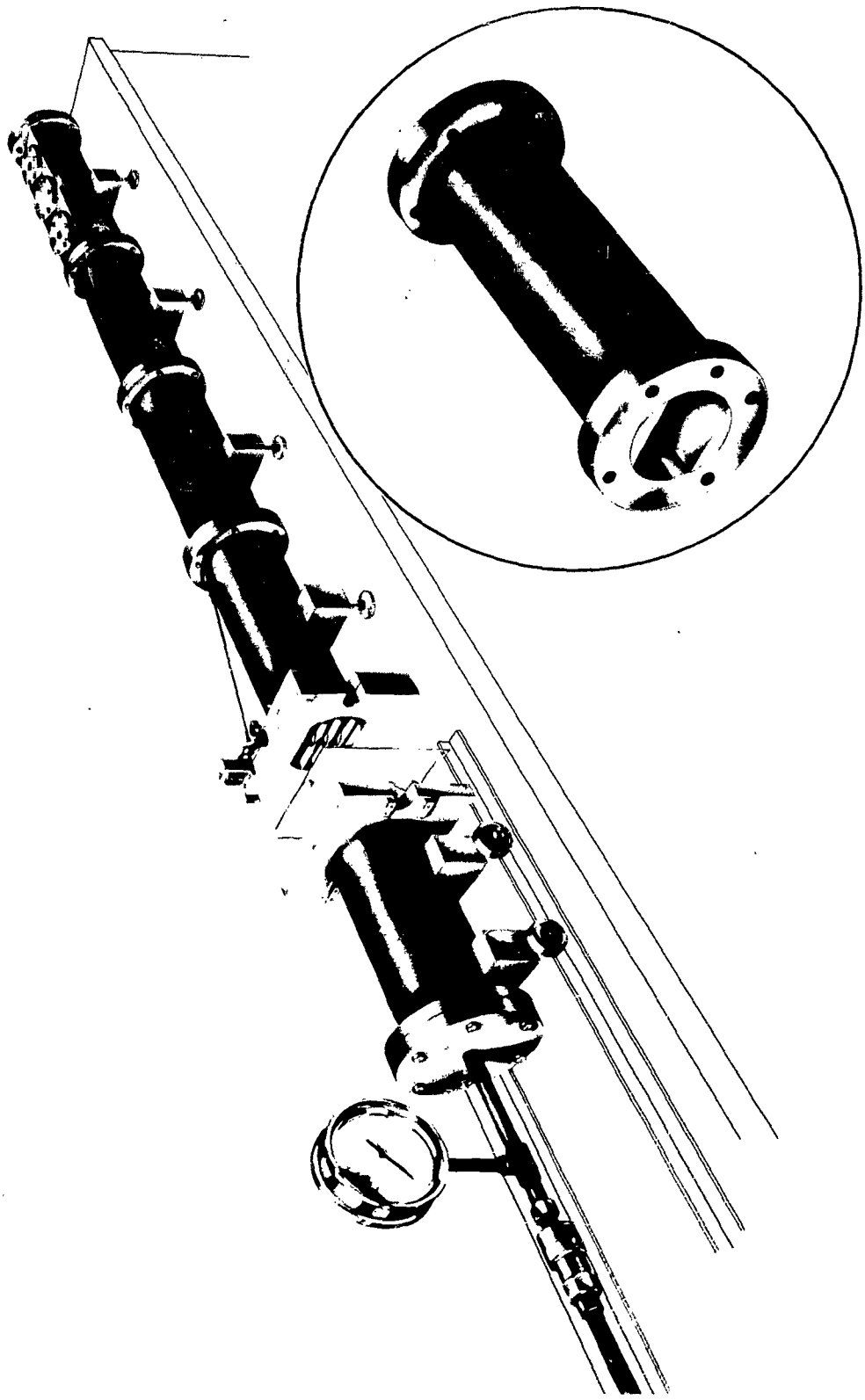

FIG. 13. Shock Tube.

Instrument Response Requirements

The pressure transient to be measured by a gage at the point of contact or at the point of stagnation for vertical entry is theoretically as follows. Upon contact, the pressure rises instantaneously to a peak value $P \simeq \rho cV$, where ρ is the density of water, c is the velocity of sound in water, and V is the velocity of the sphere. In the laboratory setup, the expected peak pressure would be about 1,600 psi and have a duration of about 1/2 μsec. After this finite interval, the pressure, according to one theory, is $P_s = \frac{1}{2}\rho V^2(0.9b^{-\frac{1}{2}} + 1 - 0.68b^{\frac{1}{2}})$ for $b < 0.1$ (for very small penetrations) where b is the penetration in radii of the sphere (Ref. 1).

It is not possible to record the instantaneous pressure rise by any gage and associated apparatus because of the finite response time. However, the decay portion of the transient, which is the portion of chief interest, can be recorded satisfactorily, at least in principle. The reproduction of the latter portion of the curve is relatively easy, but becomes increasingly difficult as one approaches the steeper portion because of the faster instrument response required. In order to reproduce the earliest portion of the curve and the peak pressure, the frequency response of the apparatus would be several megacycles. Originally, it was planned to record only the latter portion of the transient, using available gages, and to advance along the curve toward the peak as frequency response of the apparatus was improved.

Attempts To Use Available Gages

The measurement program was begun using a Dyna-Gage (Photocon Research Corp., Pasadena, Calif.). This instrument is an engine indicator of the variable-capacitance type, with a flat frequency response up to 10 kc, limited by the response of the electrical system. No reproducible records were obtained with this equipment. A Rutishauser (Rutishauser Corp., Pasadena, Calif.) gage was then obtained. This instrument is similar to the Dyna-Gage but has a much higher frequency response. It is limited, however, by the resonant frequency of the diaphragm, which, for the pressure range expected, is 100 kc. A low-pass filter was employed to limit the response to somewhat less than the diaphragm resonance frequency. A few measurements were obtained with this equipment but it was impossible to obtain reproducible results. Some of the records resembled the theoretical curves, but oscillations of considerable magnitude were superimposed on them even when a 63-kc cutoff filter was used.

Piezoelectric Gage Development

Although some usable results may have been obtained, it was decided to discontinue the use of the Rutishauser gage and attempt to obtain still higher frequency response by use of piezoelectric gages.

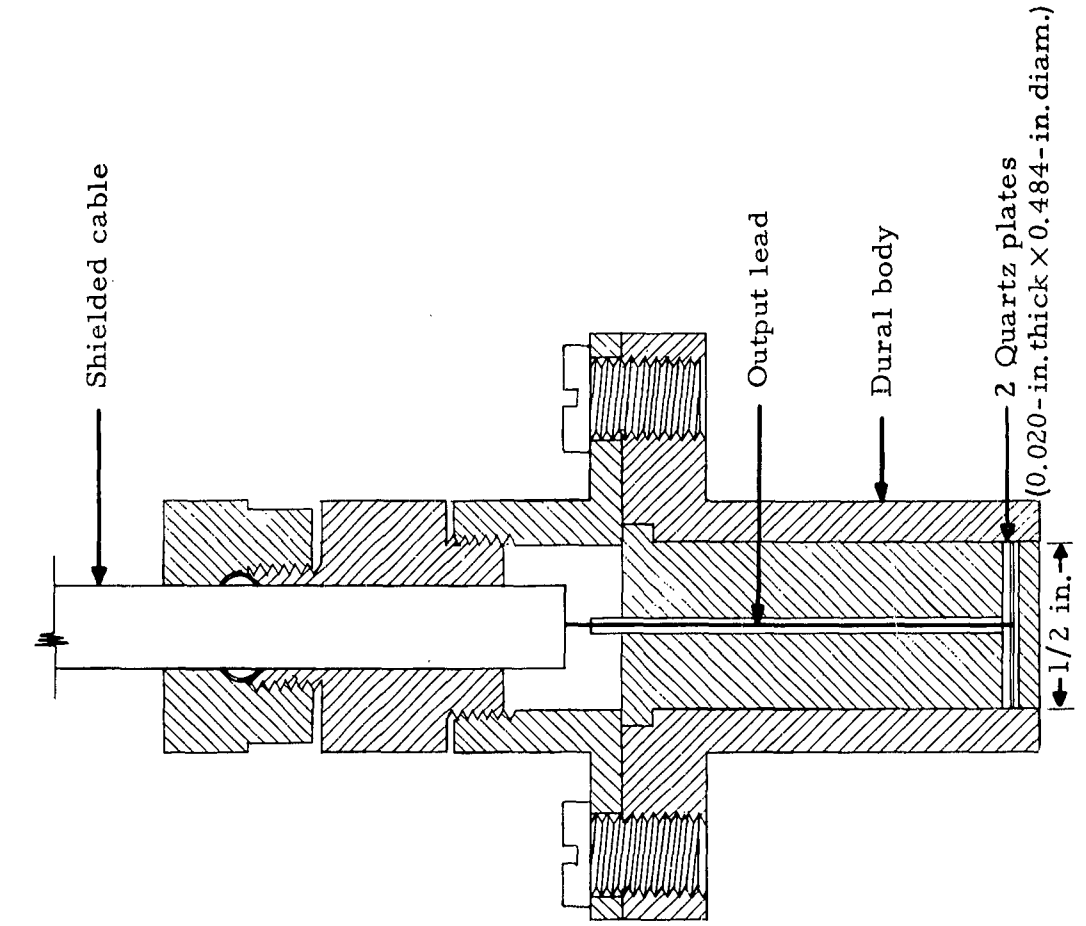

FIG. 14. Quartz Gage.

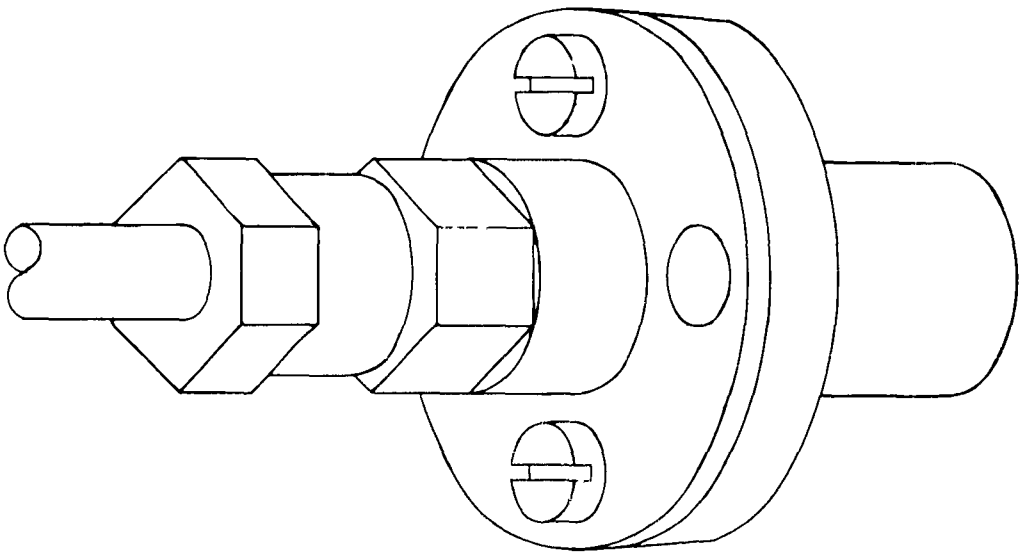

A quartz gage (Fig. 14) was constructed in the laboratory, using two X-cut plates (0.020-inch thick by 0.484-inch-diameter) sandwiched between Dural plugs. This was enclosed in a Dural housing that fitted into a hole in the hemisphere. The quartz gage made reproducible records, two of which are shown in Fig. 15a and 15b. The records do not register the peak pressure correctly but show general agreement with theory beyond about 10 μsec from impact.

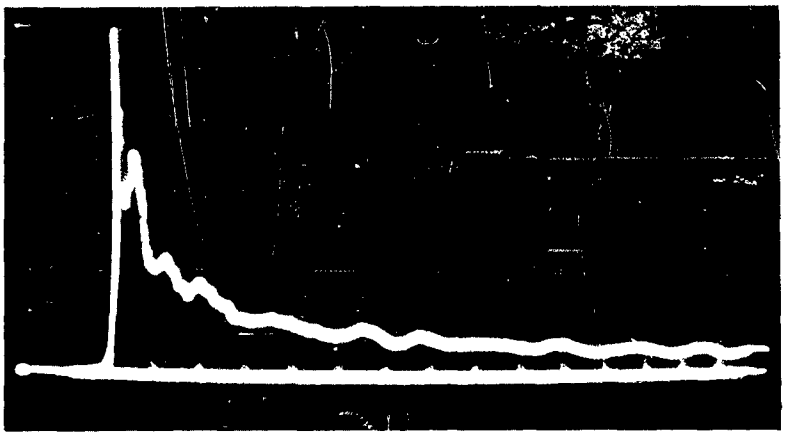

(a) Markers are 100 μsec apart.

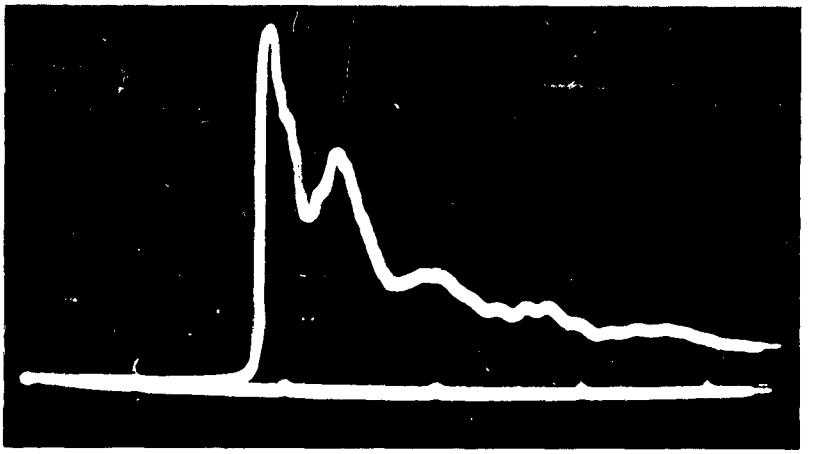

(b) Early portion of record above on a faster sweep. Markers are 100 μsec apart.

FIG. 15. Pressure Record Obtained With First Quartz Gage.

Development of "Vibrationless" Body and Gage

To eliminate elastic vibration of the experimental body (a possible cause of deviation from theory discussed below), a simple cylindrical body 1 3/4 inches in diameter and 23 inches long (Fig. 16) was substituted for the hollow hemisphere. The length is such that the time required for a stress wave to traverse it, reflect at the top, and return to the gage element is about 2×10^{-4} seconds. This permits the first 2×10^{-4} seconds of the transient to be recorded without the interfering effects of elastic vibrations of the body.

A gage consisting of a 1/2-inch-diameter rod of the same length as the body was constructed. A sensitive element of two quartz plates was inserted and cemented 1 inch from the lower end. This gage (hereafter called a rod gage) fits in the central hole of the body with a clearance to prevent radial coupling, and is attached to the body at its upper end (Fig. 16). With the lower end of the gage and body contoured to a 6-inch radius, a spherical surface is presented to a flat-water surface throughout the first 2×10^{-4} seconds (about 0.060 inch) of penetration.

Figures 17a and 17b show the response of a Dural rod gage and body to a pressure step in the shock tube. The small oscillations are presumably due to "radial" vibration (Ref. 9) of the rod at a frequency of about 240 kc. The rise time is about 3 μsec and the reflection from the opposite end appears after about 200 μsec.

Figure 18 shows the step response when the quartz is placed 0.010 inch from the end of the rod. The rise time is about 2 μsec. A comparison of Fig. 17b and 18 shows the distortion that occurs as the pulse is propagated along the rod (Ref. 9). The response was considered satisfactory for the present with the quartz 1 inch from the end. However, future development is being considered in which the quartz will be placed very close to the end. A 1/4-inch-diameter rod gage, with the quartz 1 inch from the end, was constructed with a step response showing a rise time of about 2 μsec and the "radial" vibration about 500 kc.

EXPERIMENTAL INVESTIGATION OF CAUSES OF DEVIATIONS OF EXPERIMENTAL CURVE FROM THEORY

It is possible that the irregularities in the record shown in Fig. 15 were due to various modes of vibration of the hemisphere, gage, and carriage, induced by water impact and entrapment of air between the body and the water surface. A series of experiments was begun to determine their cause, and, if possible, to eliminate them.

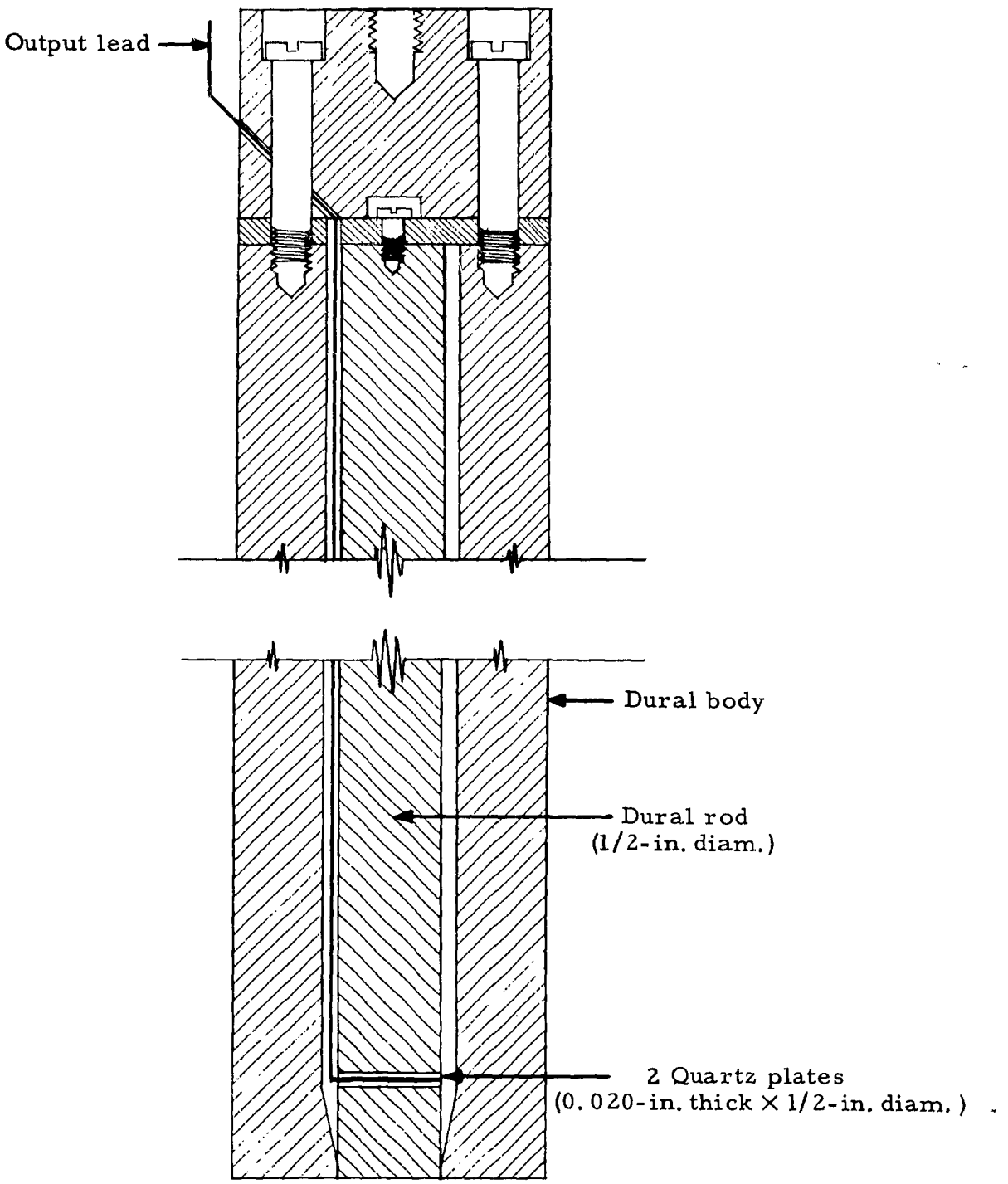

FIG. 16. Rod Gage and Body (23-Inch Length by 1 3/4-Inch Diameter).

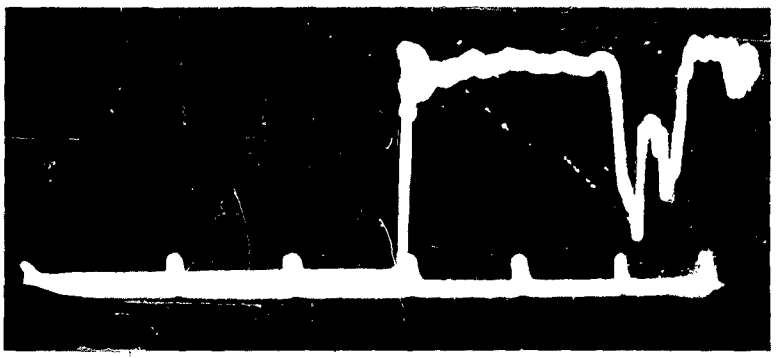

(a) Markers are 100 μsec apart.

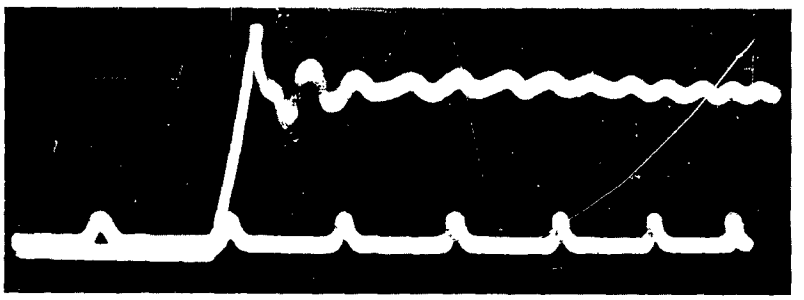

(b) Early portion of record above on a faster sweep. Markers are 10 μsec apart.

FIG. 17. Step Response of 1/2-Inch-Diameter Dural Rod Gage.

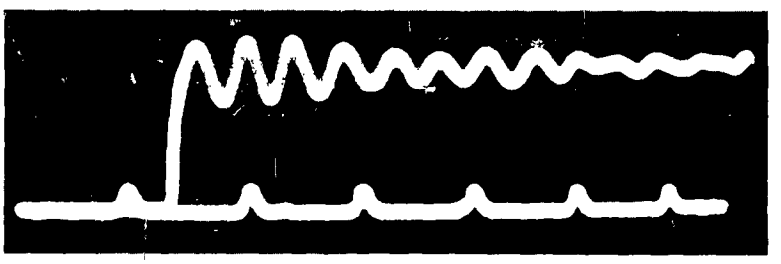

FIG. 18. Step Response of Rod Gage With Quartz Near End to Which Pressure Is Applied. Markers are 10 μsec apart.

Experiment on Effect of Elastic Vibration of the Body

A vertical column was installed inside the hemisphere with its lower end bearing on top of the gage-mounting flange and its upper end against the carriage. This column was expected to stiffen the hemisphere against its fundamental mode of vibration. Figures 19a and 19b show the result of this experiment and a comparison of Fig. 15 and 19 shows how the amplitude and character of the oscillations were altered.

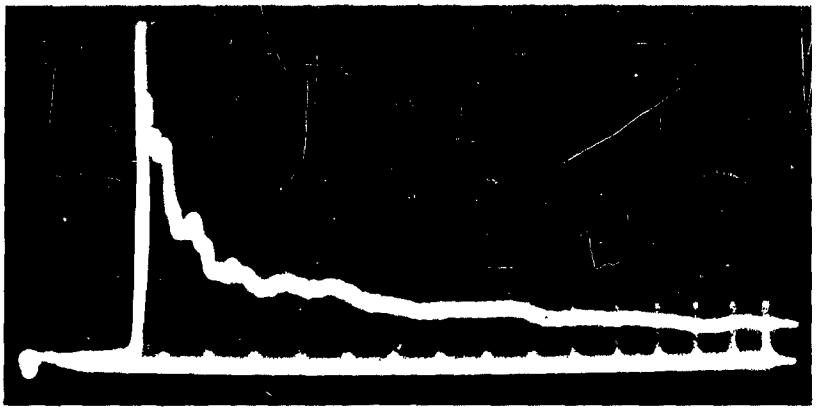

(a) Pressure record with stiffener in hemisphere. Markers are 100 μsec apart.

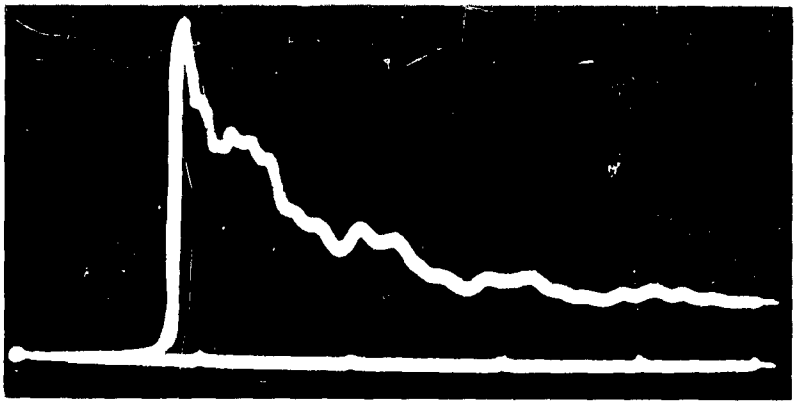

(b) Early portion of record above on a faster sweep. Markers are 100 μsec apart.

FIG. 19. Pressure Versus Time at Stagnation Point of 12-Inch Sphere.

It was learned later that pressure-time records were critically affected by the character of the gage surface and surrounding area. A slight change in the surface discontinuity at the gage installation, accidentally introduced when the vertical column was installed, could have accounted for the changes in the records. However, the cause was not known at the time and changes in the record were attributed to a change in the elastic behavior of the hemisphere and gage. Figure 20 shows a comparison of the experimental results with the column and two theoretical curves (Ref. 1).

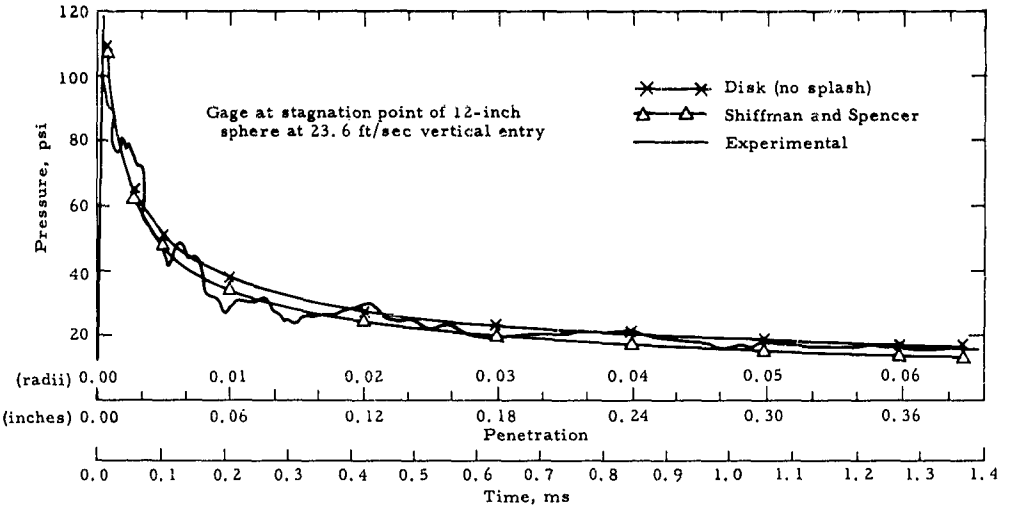

FIG. 20. Pressure Versus Time at Water Entry.

To eliminate the elastic effects, the "vibrationless" body and gage described above were substituted for the hollow hemisphere.

Figure 21 shows the records with (1) a flat end, (2) a 6-inch-radius spherical end, and (3) a 3-inch-radius spherical end. Reflections from the upper end of the rod appear after about 200 μsec.

These records, quite different from the predicted curves, were difficult to explain until it was determined that the body diameter should have been larger. Because the water surface was distorted during entry, the boundary of the spherical area affected the transient sooner than expected. Since this body did not function as expected, it was decided to return to experiments on the hollow hemisphere, and, if no satisfactory results were obtained, to use a larger cylinder.

Experiments on the Effects of Surface Defects

Another suspected cause of the deviation of experimental results from theory was the inaccuracy of contouring the gage surface. A recheck of the original setup (hollow 6-inch-radius hemisphere and

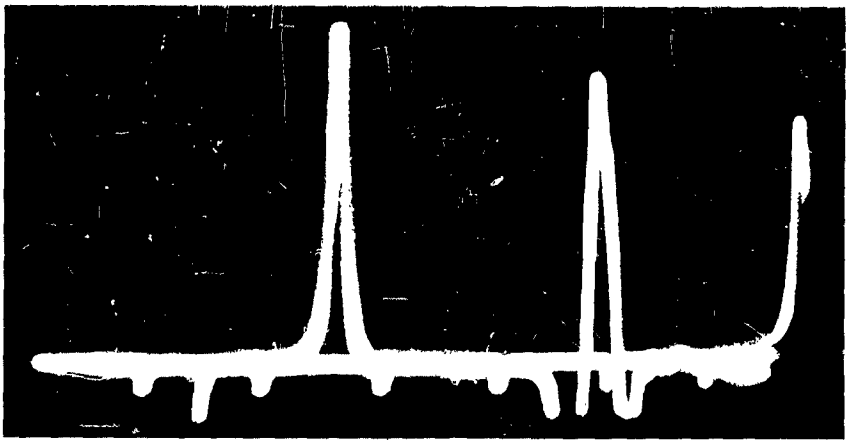

(a) Pressure at center of 1 3/4-in. diam. flat surface.

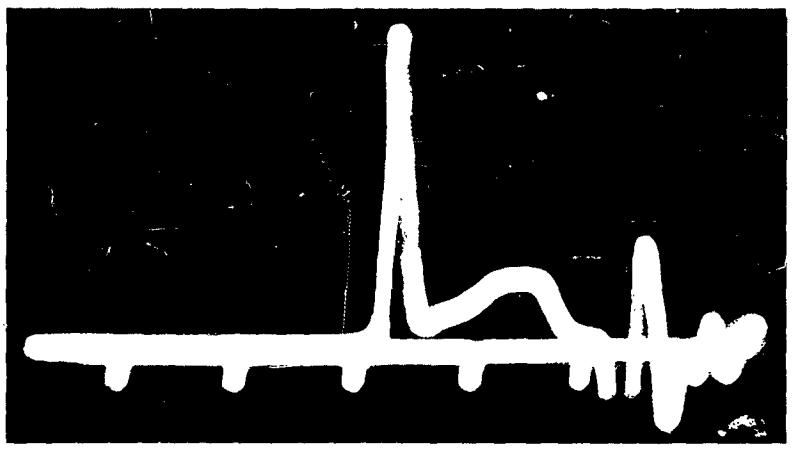

(b) Pressure at center of 1 3/4-in. diam. convex surface (6-in. radius).

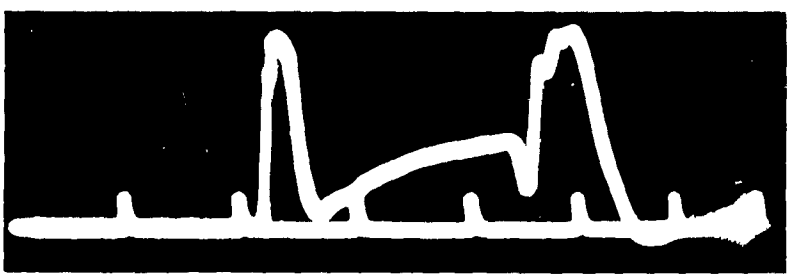

(c) Pressure at center of 1 3/4-in. diam. convex surface (3-in. radius).

FIG. 21. Pressure at Center of 1 3/4-Inch Diameter Surfaces. Markers are 100 μsec apart.

the first quartz gage, Fig. 14) was made with the gage accurately contoured. The record (Fig. 22) was similar to the original ones (Fig. 15a and 15b), but significantly different in the character of the oscillations.

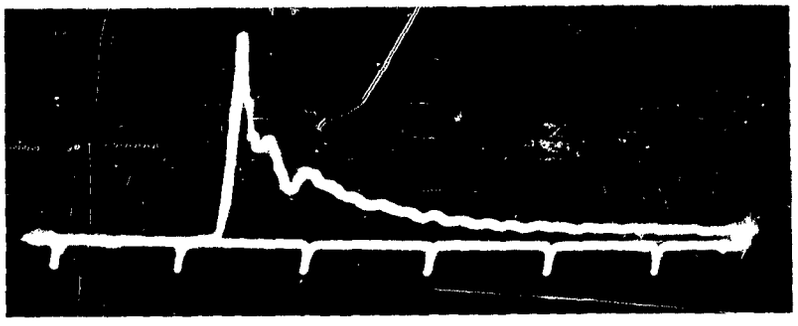

FIG. 22. Pressure Record With First Quartz Gage Accurately Contoured.

Experiments with the 1/2-inch-diameter rod gage, mounted in the hollow hemisphere, were undertaken to determine the effects of imperfections in the surface adjacent to the gage. Various imperfections were deliberately introduced and the results of each one recorded.

Figure 23a is a record with the gage protruding about 0.005 inch. Figure 23b shows a record with the gage retracted about 0.005 inch. Figure 24a shows a properly set and contoured gage with a small crack around it (approximately 0.002 inch wide). Figure 24b is the same, except for cellophane tape, which was applied over a 2-inch square covering the gage, the crack, and the surrounding area. Experiments with the 1/4-inch-diameter rod gage yielded similar results.

These experiments demonstrated that the irregularities in the records, except for the gage oscillations, were due to imperfect curvature of the gage face and surface defects surrounding the gage. When the gage is accurately contoured and set, the surface polished and covered with cellophane tape, smooth curves are obtained.

Experiment on the Effects of Trapped Air

An experiment was conducted to determine whether air was trapped between the body and the water surface during water entry, and to explore the behavior of such an air layer if it existed. An insulated Dural plug was set flush in the hemisphere in place of the pressure gage. The plug was charged to a few volts and oscillograph records of the voltage variation were obtained as the hemisphere entered the water. This voltage change is inversely proportional to change of electrical capacitance formed by the plug and the water surface. Since the capacitance depends on the separation between the plug and the water,

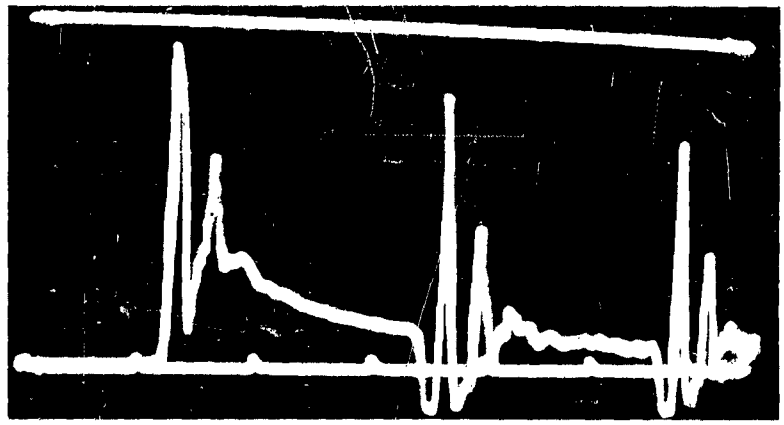

(a) Pressure record with gage protruding about 0.005 inch.

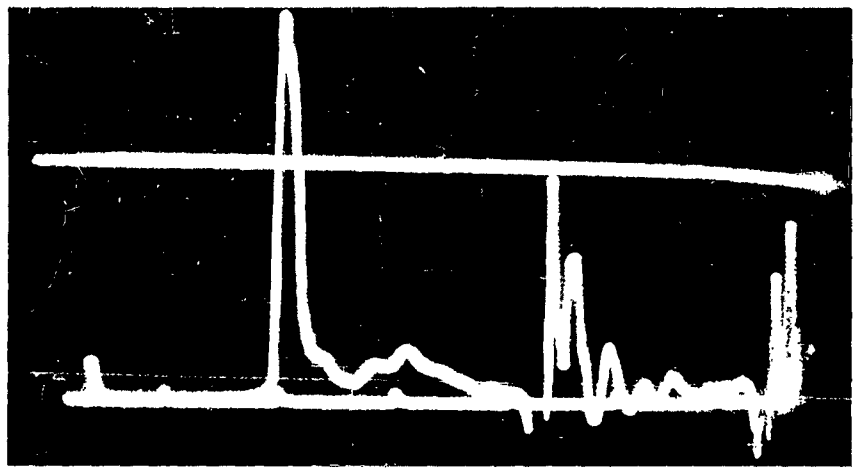

(b) Pressure record with gage retracted about 0.005 inch.

FIG. 23. Pressure Records Showing Effect at Surface Discontinuities. Markers are 100 μsec apart.

the thickness of an air layer can be deduced from the capacitance versus time measurements. (Certain simplifying assumptions must be employed, but are believed to be valid.)

A probe, attached to the carriage to strike the water just before the hemisphere entered, produced a time marker on both the pressure and capacitance records so that they could be correlated. Figure 25 shows (1) the pressure, and (2) the capacitance records made under identical conditions with the 6-inch-radius hollow hemisphere. The "gages," both capacitance and pressure, were 1/2-inch-diameter flat surfaces mounted in a 3/4-inch outside-diameter plastic bushing, which

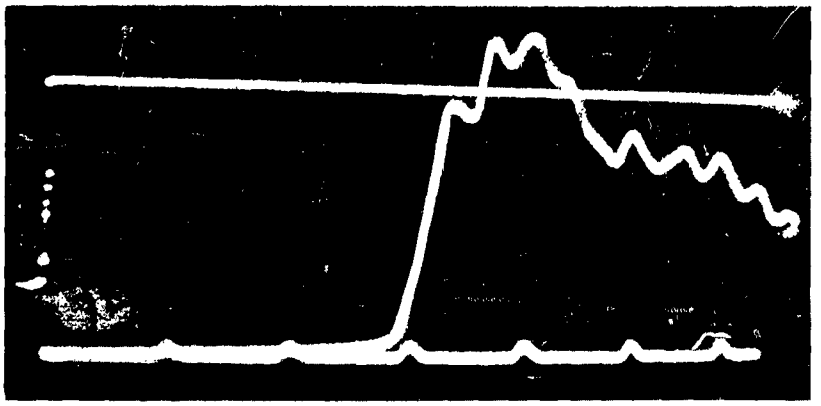

(a) Pressure record with small crack around edge.

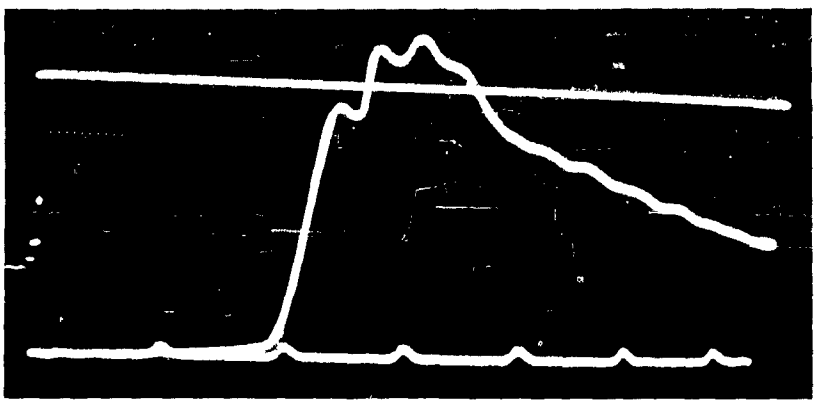

(b) Pressure record with cellophane tape over gage.

FIG. 24. Effects at Surface Smoothness. Markers are 100 μsec apart. Horizontal line equals 240 lb/psi.

also was flat on the end and flush with the gage and body surfaces. The importance of the contour was not known at the time. No quantitative analysis was attempted because of the elastic and geometric complexity of the system (flat-gage face and compliant mount), but the experiment demonstrated the existence of a trapped air layer whose presence influenced the pressure versus time variations.

RELIABLE RESULTS

After the major difficulties in the experimental work were resolved; namely, the development of fast response gages and the perfection of surfaces and fits, the records in Fig. 26a and 26b were

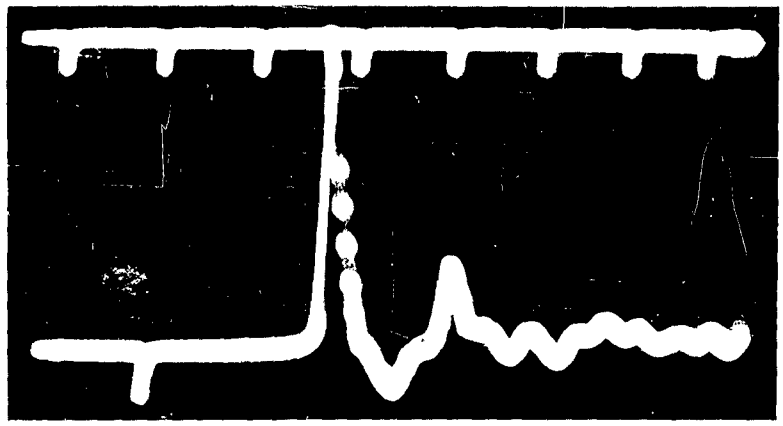

(a) Pressure.

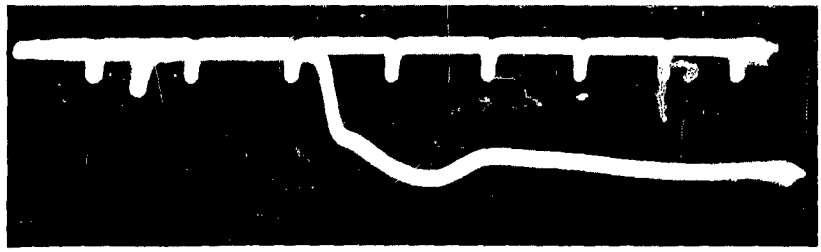

(b) Reciprocal of capacitance - a function of air-layer thickness.

FIG. 25. Correlation of Pressure and Air-Layer Thickness. Markers are 100 μsec apart.

made. To obtain these records, the 1/2-inch-diameter rod gage was used at the stagnation point of the hollow 6-inch-radius Dural hemisphere. The small oscillations are due to "radial" vibration of the rod. Figures 27a and 27b show similar results obtained with a 1/4-inch-diameter rod gage. Figure 28 is a plot of the experimental results with a smooth curve drawn through the mean of the gage oscillations. These points were obtained from two records on each gage; one using a fast sweep to resolve the initial portion, and a second one using a slower sweep to obtain the later portion of the decay.

Since a gage has a finite area, it registers total force on its sensitive face rather than pressure at a point. For comparison, theoretical curves of total force versus time on the gage are also plotted in Fig. 28. These curves were derived by integrating over the gage area the expanding disk expression of E. P. Cooper reported in Ref. 1. They start at the time the entire gage face is theoretically immersed. Because of the trapped air that gradually escapes, the instant of

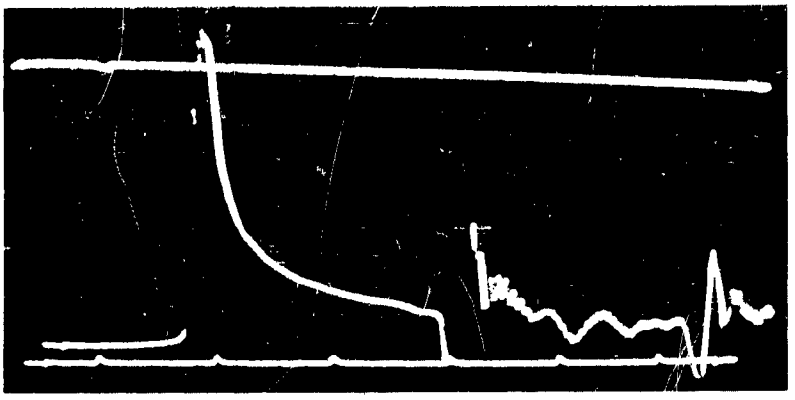

(a) Horizontal line equals 240 lb/psi. Markers are 100 μsec apart.

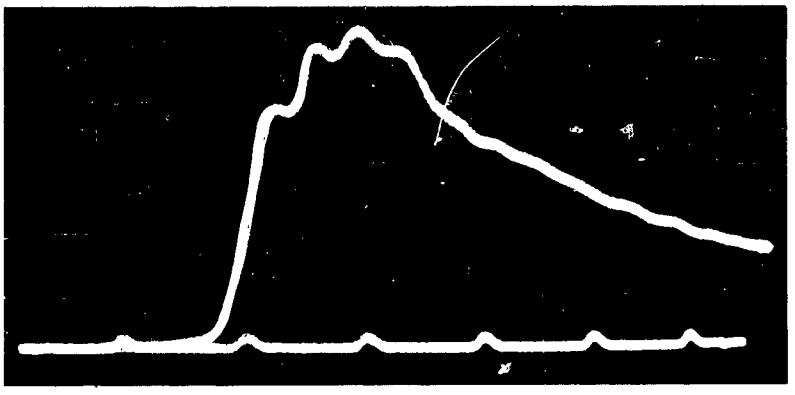

(b) Early portion of record above on a faster sweep. Markers are 10 μsec apart.

FIG. 26. Pressure Records Obtained With 1/2-Inch Diameter Rod Gage at Stagnation Point on 6-Inch Radius Hemisphere.

impact is not sharply defined. However, for purposes of comparing theory with experiment, impact was assumed to occur at the time the pressure began to rise very rapidly, although a gradual pressure rise beginning several microseconds earlier is discernible.

CONCLUSIONS

1. Instrument development has progressed sufficiently to permit satisfactory recording of the pressure transients obtained in the laboratory. Presumably, the instruments will function satisfactorily in planned range tests at 80 ft/sec entry velocity.

(a) Markers are 100 μsec apart.

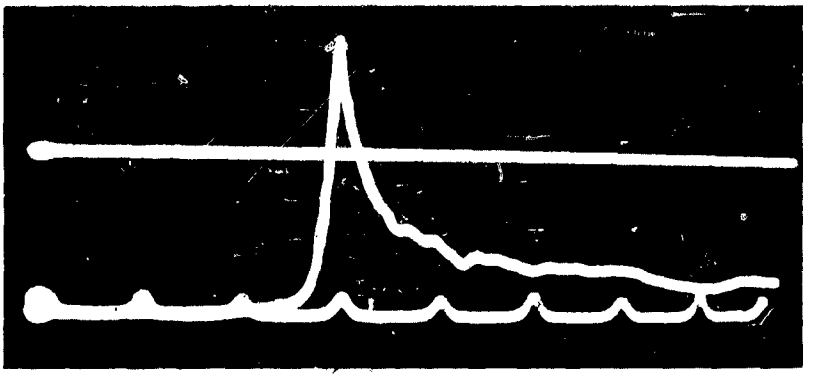

(b) Early portion of record above on a faster sweep. Markers are 10 μsec apart.

FIG. 27. Pressure Records Obtained With 1/4-Inch Diameter Rod Gage. Horizontal line equals 375 psi.

2. Tentatively, the discrepancy between theory and experiment may be attributed to the presence of air, which is trapped between the water surface and the body and forms a cushion; this reduces the peak pressure and deforms the decay curve. Before any accurate check on the validity of the theory is possible, it may be necessary to eliminate the air as nearly as possible.

PROGRAM OF WORK

Gage Development. Work on improved gage design is being directed toward higher frequency response without the limitation on total transient length imposed by the rod gage. Attempts are also being made to improve the signal-to-noise ratio of the gage, to decrease the size, and to improve the method of mounting and of sealing the surface around the gage.

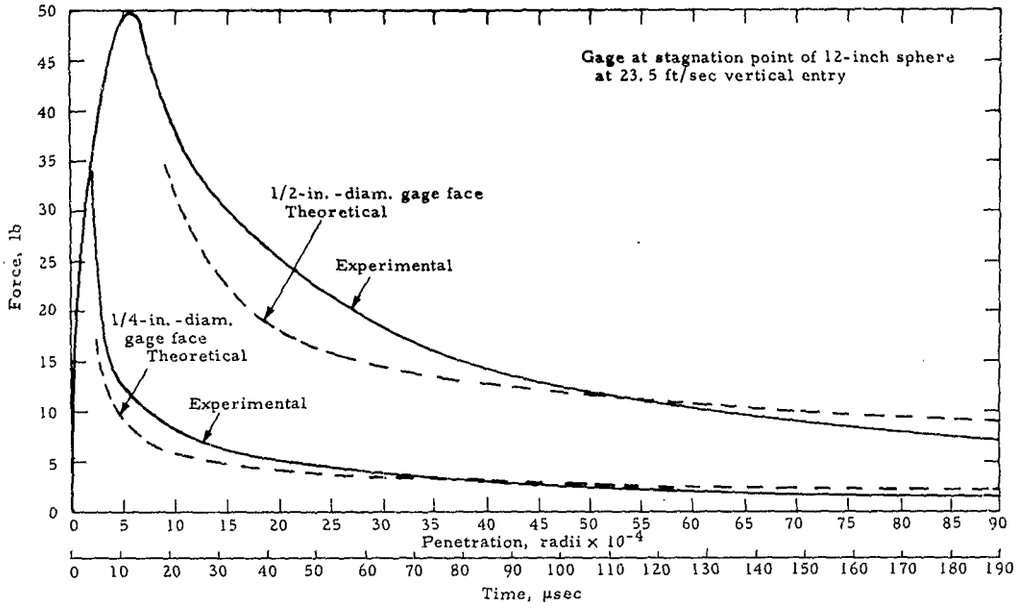

FIG. 28. Force Versus Time at Water Entry.

Range Tests. Initial range tests are in preparation, consisting of dropping a test body from heights of 150 feet into the water at the Morris Dam Range. These drops will test the suitability of present gages for use at higher velocities and under field conditions, in addition to contributing useful data.

The signal will be conveyed to shore-based recording equipment via a trailing cable. Both vertical and oblique tests are planned, and gages will be installed at various points on the 12-inch-diameter spherical nose of the body.

Laboratory Tests. It is tentatively planned to study the effects of gas above the water surface by using an enclosed apparatus in which the atmosphere can be controlled.

Theoretical Work. An attempt will be made to modify present theory to include the effects of the atmosphere on the pressure curve. This will have practical significance if experiment shows that the atmospheric effect is important at high velocities.

The practical significance of the fine structure of the pressure curve, especially the high initial spike as it affects structural and ballistic problems, has been questioned. Therefore it seems desirable to investigate theoretically this detail and attempt to determine its significance to the relationship.

REFERENCES

1. U. S. Naval Ordnance Test Station, Inyokern. Pressure Distribution on a Sphere Entering Water Based on Various Linearized Theoretical Models, by Robert H. Korkegi. China Lake, Calif., NOTS, 13 September 1950. (NOTS Technical Memorandum 808-40.)

2. New York University. The Force of Impact on a Sphere Striking a Water Surface, by M. Shiffman and D. C. Spencer. New York, NYU, February 1945. (AMP Report 42.1R. AMG-NYU No. 105.)

3. _____. The Force of Impact on a Sphere Striking a Water Surface, by M. Shiffman and D. C. Spencer. New York, NYU, July 1945. (AMP Report 42.2R. AMG-NYU No. 133.)

4. U. S. Naval Ordnance Test Station, Inyokern. Theoretical Considerations of Proposed Water-Entry Pressure Measurements, by E. P. Cooper. Inyokern, Calif., NOTS, 8 November 1949. (NOTS Technical Memorandum, NP45-5001/A9-16.)

5. Szebehely, V. G. "Hydrodynamic Impact," APPL MECH REV, Vol. 12, No. 5 (May 1959).

6. Birkhoff, Garrett. "Jets, Wakes and Cavities." ONR Symposium on Naval Hydrodynamics, Washington. 25 - 29 August 1958.

7. U. S. Naval Ordnance Test Station, Inyokern. The Compressional Shock Due to the Impact of a Body on a Plane Water Surface, by L. Trilling. China Lake, Calif., NOTS, 13 September 1950. (NOTS Technical Memorandum 808-39.)

8. Office of Scientific Research and Development. Final Report on the Shock Tube, Piezoelectric Gages, and Recording Apparatus, by J. C. Fletcher and others. Washington, OSRD, February 1946. (OSRD 6321.)

9. Davies, R. H. "Critical Study of the Hopkinson Pressure Bar," in Royal Society of London Philosophical Transactions, Series A, Vol. 240, p. 375.

INITIAL DISTRIBUTION

4 Chief, Bureau of Naval Weapons
  DLI-31 (2)
  RU (1)
  RUTO (1)
1 Chief of Naval Research (Code 104)
1 David W. Taylor Model Basin
1 Naval Air Development Center, Johnsville
1 Naval Ordnance Laboratory, White Oak
1 Naval Postgraduate School, Monterey (Library, Technical Reports Section)
2 Naval Research Laboratory
  Code 5550 (1)
1 Naval Torpedo Station, Keyport (Quality Evaluation Laboratory, Technical Library)
1 Naval Underwater Ordnance Station, Newport
2 Naval Weapons Services Office, Naval Weapons Plant
1 Navy Electronics Laboratory, San Diego
1 Navy Underwater Sound Laboratory, Fort Trumbull
10 Armed Services Technical Information Agency (TIPCR)
1 Applied Physics Laboratory, University of Washington, Seattle
1 Hudson Laboratories, Columbia University, Dobbs Ferry, N. Y.
1 Ordnance Research Laboratory, Pennsylvania State University (Development Contract Administrator)
1 Scripps Institution of Oceanography, University of California, La Jolla (Document Control)
1 Woods Hole Oceanographic Institution, Woods Hole, Mass.

ABSTRACT CARD

U. S. Naval Ordnance Test Station
Experimental Determination of Pressure Distribution on a Sphere During Water Entry, by C. R. Nisewanger. China Lake, Calif., NOTS, 27 October 1961. 38 pp. (NAVWEPS Report 7808, NOTS TP 2806), UNCLASSIFIED.

ABSTRACT. The pressure distribution on a 12-inch-diameter sphere during vertical water entry at 23.5 fps was determined by direct pressures versus time measurements at several points on the sphere.

(Over)
1 card, 4 copies

U. S. Naval Ordnance Test Station
Experimental Determination of Pressure Distribution on a Sphere During Water Entry, by C. R. Nisewanger. China Lake, Calif., NOTS, 27 October 1961. 38 pp. (NAVWEPS Report 7808, NOTS TP 2806), UNCLASSIFIED.

ABSTRACT. The pressure distribution on a 12-inch-diameter sphere during vertical water entry at 23.5 fps was determined by direct pressures versus time measurements at several points on the sphere.

(Over)
1 card, 4 copies

U. S. Naval Ordnance Test Station
Experimental Determination of Pressure Distribution on a Sphere During Water Entry, by C. R. Nisewanger. China Lake, Calif., NOTS, 27 October 1961. 38 pp. (NAVWEPS Report 7808, NOTS TP 2806), UNCLASSIFIED.

ABSTRACT. The pressure distribution on a 12-inch-diameter sphere during vertical water entry at 23.5 fps was determined by direct pressures versus time measurements at several points on the sphere.

(Over)
1 card, 4 copies

U. S. Naval Ordnance Test Station
Experimental Determination of Pressure Distribution on a Sphere During Water Entry, by C. R. Nisewanger. China Lake, Calif., NOTS, 27 October 1961. 38 pp. (NAVWEPS Report 7808, NOTS TP 2806), UNCLASSIFIED.

ABSTRACT. The pressure distribution on a 12-inch-diameter sphere during vertical water entry at 23.5 fps was determined by direct pressures versus time measurements at several points on the sphere.

(Over)
1 card, 4 copies

NAVWEPS Report 7808

From these data, pressure versus angle from the stagnation point was plotted for various penetrations; the rise of the free surface of the water versus penetration was determined; and the drag coefficient versus penetration was ascertained by graphic integration of the pressure-distribution curves and by acceleration measurement.

The results are compared with some theoretical curves.

NAVWEPS Report 7808

From these data, pressure versus angle from the stagnation point was plotted for various penetrations; the rise of the free surface of the water versus penetration was determined; and the drag coefficient versus penetration was ascertained by graphic integration of the pressure-distribution curves and by acceleration measurement.

The results are compared with some theoretical curves.

NAVWEPS Report 7808

From these data, pressure versus angle from the stagnation point was plotted for various penetrations; the rise of the free surface of the water versus penetration was determined; and the drag coefficient versus penetration was ascertained by graphic integration of the pressure-distribution curves and by acceleration measurement.

The results are compared with some theoretical curves.

NAVWEPS Report 7808

From these data, pressure versus angle from the stagnation point was plotted for various penetrations; the rise of the free surface of the water versus penetration was determined; and the drag coefficient versus penetration was ascertained by graphic integraion of the pressure-distribution curves and by acceleration measurement.

The results are compared with some theoretical curves.